

PREDICTION OF LIQUID HOLDUP FOR A MULTI-PLANE SYSTEM USING ARTIFICIAL NEURAL NETWORK

A thesis presented to the Department of Petroleum Engineering

African University of Science and Technology

In partial fulfilment of the requirements for the degree of

MASTER OF SCIENCE IN PETROLEUM ENGINEERING

By

Saliu Halima

Supervised by

Prof. Mukhtar Abdulkadir



African University of Science and Technology

www.aust.edu.ng

P.M.B 681, Garki, Abuja

F.C.T Nigeria

December, 2020

CERTIFICATION

This is to certify that the thesis titled “**PREDICTION OF LIQUID HOLDUP FOR A MULTI-PLANE SYSTEM USING ARTIFICIAL NEURAL NETWORK**” submitted to the school of postgraduate studies; African University of Science and Technology (AUST), Abuja, Nigeria for the award of the Master's degree is a record of original research carried out by SALIU HALIMA in the Department of Petroleum Engineering.

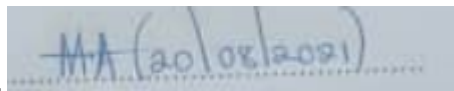
PREDICTION OF LIQUID HOLDUP FOR A MULTI-PLANE SYSTEM USING ARTIFICIAL
NEURAL NETWORK

By

SALIU HALIMA

A THESIS APPROVED BY THE PETROLEUM ENGINEERING DEPARTMENT

RECOMMENDED:

.....


Supervisor, Prof. Mukhtar Abdulkadir

.....
Co-Supervisor,

Co-Supervisor,

.....


Head, Department of Petroleum Engineering

APPROVED:

.....
Chief Academic Officer

.....
Date

© 2020
Saliu Halima

ALL RIGHTS RESERVED

ABSTRACT

Liquid holdup was predicted for slug flow using the neural network toolbox available in MATLAB. Experimental data contained Liquid holdup measured at an interval of 5 seconds over a period of 12,000 time points for both planes of a horizontal pipe setting. 13 different gas superficial velocities were varied (within a range of 0.05-4.73 m/s) while keeping the liquid superficial velocity constant for three different cases. The neural network's efficiency was analyzed by comparing experimental and simulated values of average liquid holdup. The neural network proved to be highly efficient as close similarities were observed for all values of average liquid holdup for both cases. The neural network's efficiency was further ascertained by the analysis of the "Error Autocorrelation chart " which showed the error at all other lags (asides from the zero lag) lying within the confidence limit for all cases considered. Computational macros were used to determine the structural velocity and frequency for both experimental and simulated run(s). A cross plot of simulated and experimental values for these parameters gave a very good fitting; further emphasizing the efficiency of the neural network as a tool for this research.

The effect of gas and liquid superficial velocities on liquid holdup was also investigated. It was observed that the liquid holdup decreased with increasing gas superficial velocity and increased with increasing liquid superficial velocity. This could be attributed to the increase in the gas phase residence time with an increase in gas superficial velocity, thereby reducing the fraction of fluid available for the liquid phase and thus, the liquid holdup.

Keyword: Neural network, Liquid holdup.

ACKNOWLEDGEMENT

I want to acknowledge the efforts of my parents during the course of this work and my stay at AUST. Their words of encouragement, love, care and support have brought me this far and I am forever indebted to them.

To my loving husband, words alone cannot describe how much I appreciate your support, love and concern all through my program. You have always been there from the start. I remain indebted to you my love.

To my siblings; Abubakar, Amina, Abdulaziz, Abdulsalam and Abdulraheem. I appreciate your immense support and love all through my program.

To my supervisor Prof. Mukhtar Abdulkadir, your supervisory role and guidance towards the completion of this work cannot be overemphasized. You were always ready to help out and put me through whenever I faced challenges. Your contributions, positive criticism and efforts are greatly appreciated.

I wish to acknowledge the energy, time and effort of the Head of Department; Prof. Alpheus Igbokoyi and the entire staff of AUST in making us better than we use to be. I really appreciate.

Special thanks to my course mate Kawu Musa Idris who took time to put me through the basics of artificial neural network. I also want to thank ex-students; Fawziyah Olarinoye and Isah Muhammed for their constant support and encouragement all through this programme.

Finally, I wish to appreciate my friends on campus; Solomon Israel Sunday, Damilola Ibrahim, Raji Kauthar, Oluwaseun Alonge and all those I can't mention here for their support and words of encouragement all through my stay at AUST.

DEDICATION

This research is dedicated to the Almighty Allah, my wonderful parents, my loving husband, my beautiful baby girl, my supportive siblings and my amiable friends.

TABLE OF CONTENT

CHAPTER 1: INTRODUCTION

1.1. Background	13
1.2. Review of Literature	14
1.3. Problem Statement.....	15
1.4. Objective of Research.....	15
1.5. Organization of Research.....	15

CHAPTER 2: LITERATURE REVIEW

2.1. Definition of Gas-Liquid Flow.....	17
2.2. Flow Regime.....	19
2.3. Flow Pattern Identification Techniques.....	23
2.4. Flow Pattern Maps.....	23
2.5. Predictive Modelling.....	24
2.6. Activation Function.....	27
2.7. ANN Architecture.....	28
2.8. Methods of adjusting weights.....	28
2.9. ANN Training Process.....	29
2.10. ANN Validation Process.....	30
2.11. ANN Testing Process.....	31
2.12. Review of Past Work on the Prediction of Liquid Holdup in a Horizontal Pipe.....	31

CHAPTER 3: METHODOLOGY

3.1. Data Acquisition.....	34
3.2. Data Processing.....	34
3.3. Predictive Model Selection.....	34
3.4. Training of Neural Network.....	35
3.5. Evaluation of Model.....	41
3.6. Determination of Structural Velocity and Frequency.....	42

CHAPTER 4: RESULTS/DISCUSSION OF RESULTS

4.1. Analysis Based on MATLAB Charts and Tables.....	43
4.2. Analysis based on average liquid holdup.....	54
4.3. Analysis based on structural velocity and frequency.....	58
CHAPTER 5: CONCLUSION/RECOMMENDATION	
5.1.CONCLUSION.....	61
5.2 RECOMMENDATION.....	61
REFERENCES.....	63

LIST OF FIGURES

Figure 2.1- Flow regime types for horizontal flow pipe.....	21
Figure 2.2- Flow Regime Types for Vertical Pipes.....	23
Figure 2.3- Brain neuron.....	26
Figure 2.4-Model of an artificial neuron.....	26
Figure 2.5-Sigmoid Function.....	27
Figure 3.1: Selecting the NARX as a solution to the time series problem.....	35
Figure 3.2-Importation of time series data.....	36
Figure 3.3-Splitting time series data set for training, validation and testing.....	36
Figure 3.4-Architecture of Neural Network.....	37
Figure 3.5- Training Algorithm Selection.....	41
Figure 3.6- Training the neural network.....	42
Figure 3.7-Autocorrelation of Error 1 chat.....	43
Figure 4.1- Autocorrelation of error 1 plot for plane 1 (USL=0.05 m/s, USG=0.05 m/s).....	45
Figure 4.2- Autocorrelation of error 1 plot for plane 1 (USL=0.09 m/s, USG=0.05 m/s).....	45
Figure 4.3- Autocorrelation of error 1 plot for plane 1 (USL=0.14 m/s, USG=0.05 m/s).....	46
Figure 4.4- Autocorrelation of error 1 plot for plane 2 (USL=0.05 m/s, USG=0.05 m/s).....	46
Fig 4.5- Autocorrelation of error 1 plot for plane 2 (USL=0.09 m/s, USG=0.05 m/s).....	47
Figure 4.6- Auto correlation of error 1 plot of for plane 2 (USL=0.14 m/s, USG=0.05 m/s)....	47
Figure 4.7- Performance plot for plane 1 (USL=0.05 m/s, USG=0.54 m/s).....	48
Figure 4.8- Performance plot for plane 1 (USL=0.09 m/s, USG=0.54 m/s).....	49
Figure 4.9- Performance plot for plane 1 (USL=0.14 m/s, USG=0.54 m/s).....	49
Figure 4.10-Time series plot for plane 1 (USL=0.05 m/s and USG=0.05 m/s).....	54
Figure 4.11- Time series plot for plane 1 (USL=0.09 m/s and USG=0.05 m/s).....	54
Figure 4.12- Time series plot for plane 1 (USL=0.14 m/s and USG=0.05 m/s).....	55
Figure 4.13- Plot of Liquid Holdup versus Gas superficial Velocity (experimental).....	59
Figure 4.14- Plot of Liquid Holdup versus Gas Superficial Velocity (simulated).....	60
Figure 4.15- Crossplot of simulated and experimental structural velocities.....	61
Figure 4.16- Crossplot of experimental and simulated frequencies.....	61
Figure 4.17- Plot of Structural velocity (experimental) versus Liquid superficial velocity.....	62

Figure 4.18- Plot of Structural velocity (simulated) versus Liquid superficial velocity.....62

LIST OF TABLES

Table 3.1- Neural Network Specification for each gas and liquid superficial velocity for plane 1.....	38
Table 3.2- Neural Network Specification for each gas and liquid superficial velocity for plane 1.....	40
Table 4.1- Mean squared error (MSE) values for plane 1 (USL=0.05 m/s).....	50
Table 4.2- Mean squared error (MSE) values for plane 1 (USL=0.09 m/s).....	51
Table 4.3- Mean squared error (MSE) values for plane 1 (USL=0.14 m/s).....	51
Table 4.4- Mean squared error (MSE) values for plane 2 (USL=0.05 m/s).....	52
Table 4.5- Mean squared error (MSE) values for plane 2 (USL=0.09 m/s).....	52
Table 4.6- Mean squared error (MSE) values for plane 2 (USL=0.14 m/s).....	53
Table 4.7- Average liquid holdup for experimental and simulated run(s) for plane 1 (USL=0.05 m/s).....	56
Table 4.8- Average liquid holdup for experimental and simulated run(s) for plane 1 (USL=0.09 m/s).....	56
Table 4.9- Average liquid holdup for experimental and simulated run(s) for plane 1 (USL=0.14m/s).....	57
Table 4.10- Average liquid holdup for experimental and simulated run(s) for plane 2 (USL=0.05 m/s).....	57
Table 4.11- Average liquid holdup for experimental and simulated run(s) for plane 2 (USL=0.09 m/s).....	58
Table 4.12- Average liquid holdup for experimental and simulated run(s) for plane 1 (USL=0.14 m/s).....	58

CHAPTER ONE

INTRODUCTION

1.1. BACKGROUND

Multiphase flow is defined as the simultaneous flow of a mixture comprising two or more phases. This could be a combination of liquid/liquid, liquid/solid, gas/solid and gas/liquid flow. Two phase flow in pipes is a fundamental aspect of multiphase flow encountered in a wide range of industrial processes. These include the chemical, petroleum, process, power generation, refrigeration and nuclear industries. The application of multiphase flow is of great importance in condensers, evaporators, boilers, distillation towers, nuclear power plants, boilers, crude oil transportation and chemical plants, among others.

Key parameters encountered in the design of any multiphase system includes the mass flowrate, volumetric flowrate, mass flux, flow velocities, phase fraction (liquid holdup and void fraction), pressure drop prediction and estimation, convective heat transfers distribution term, slip values among others. Flow regimes prediction and identification is also an important concept to be considered in designing a multiphase system.

The parameter which describes the rate at which fluid is released in a pipe according, to (Xiao et al., 2020), is the liquid holdup. The liquid holdup is the ratio of the liquid phase in the flow area to the total flow area of interest. As a result of changes in fluid temperature and pressure, the values of liquid holdup are not constant along the pipe length.

The liquid holdup is a parameter that holds a significant part in predicting pressure drop-in two-phase flow, sizing of process and control equipment such as slug catchers, separator, two-phase pumps and control valves.

From the investigations carried out by (Beggs & Brill, 1973), the influential factors which influence liquid holdup in a horizontal pipe include the pipe diameter, liquid-phase superficial velocity, gas-phase superficial velocity, pressure, viscosity and temperature. Some of these factors are examined in Chapter 4.

The applicability of these methods is usually restricted by their failure to consistently deliver results with high accuracy.

Technological advancement in science and technology has led to the utilization of artificial intelligence algorithms such as artificial neural networks in the oil and gas industry. Artificial intelligence (AI) works based on the concept that human intelligence can be defined in a way

that makes it easy for a machine to imitate and carry out given tasks effectively (Frankenfield, 2021). A key aspect of AI is machine learning. In machine learning, computer programs automatically learn and adapt to new data with little or no assistance from humans (Frankenfield, 2021). Researchers in the field of artificial intelligence according to, (Frankenfield, 2021), have recorded remarkable success in imitating activities which includes learning and reasoning. There is no limit to the application of artificial intelligence as a tool for a wide range of industries.

An artificial neural network (ANN) is an imitation of the human brain (Harvey & Harvey, 1998). An artificial neural network comprises processing units called neurons. As a result of their ability to effectively carry out both easy and complicated computational tasks, interest in models of artificial neural networks (ANN) has increased recently (Vrahatis et al., 2001). ANNs develop their functionality based on training (sampled) data. A neural network learns how to efficiently minimize a cost function defined as the multivariable error function of the network. It achieves this through the development of efficient learning algorithms. The task of minimizing a function is well-known in the field of numerical analysis

Prediction is a type of dynamic filtering in which past values of one or more-time series are employed to predict future ones. On the other hand, predictive modelling, according to (Frankenfield, 2019), involves the use of known results to generate, process and validate a model that can be utilised to forecast or predict future outcomes. Predictive models are constructed and widely applied over time for analysis, simulation, monitoring and control of a wide range of systems such as chemical processes, manufacturing processes, aerospace technology, and robotics, among others.

A dynamic neural network that consists of tapped delay lines is utilised for nonlinear filtering and prediction. A neural network tool solves a time series problem by predicting subsequent values of one-time series given another time series. It carries out this prediction by employing the use of only one of the series for less complex systems or both series for a more accurate result.

1.2. PROBLEM STATEMENT

Sound knowledge of liquid holdup is required to understand two-phase gas-liquid flow systems. The parameter is a significant feature of any gas-liquid flow system, regardless of the type of flow pattern of interest or pipe orientation, be it horizontal, vertical or inclined. The prediction of this parameter in a horizontal pipeline is of particular interest to the oil and gas industry since most of the fluid flow encountered in this area is multiphase. Also, a good understanding of this parameter is essential for the proper design of surface facilities in both onshore and offshore fields

1.3. AIMS AND OBJECTIVES OF THE RESEARCH

Aims

The aim of this research is to apply the use of the neural network system via MATLAB to predict liquid holdup during slug flow in a horizontal pipeline system.

Objectives

The aim of this research would be achieved through the following objectives:

- i. Processing, analyzing and interpreting of raw experimental data
- ii. Training a neural network via MATLAB using the experimental data, to predict liquid hold up during slug flow for a horizontal pipe orientation.
- iii. Validate the output or results obtained from the neural network via the use of MATLAB charts, tables and comparing results obtained from the neural network with the raw experimental data.
- iv. Investigate the effect of liquid and gas superficial velocities on liquid holdup, structural velocity and slug frequency.

1.4. JUSTIFICATION OF RESEARCH

The use of the neural network is imperative for predicting the liquid holdup for slug flow in a horizontal pipe with high accuracy within a shorter time frame. This would assist in more time and cost savings compared to when the other available method(s) of doing this are employed. The present study will also enrich the existing literature on horizontal flow in pipes and also provide opportunities for research in the area of neural network.

1.5. ORGANIZATION OF RESEARCH

The report is structured in this format;

- Chapter one contains the introduction of the topic, explains why the research is being carried out and highlights the aim and the objectives of the research.
- Chapter two is the review of previous researches on two-phase flow, flow regimes for different pipe orientations, flow pattern identification techniques, predictive modeling and method of operation of artificial neural network. This chapter also highlights research work which has been carried out in this area and their findings.
- Chapter three highlights the methodology applied to achieve the set the objectives for this research work. This includes consisting of data acquisition, data processing, predictive model selection and application and model evaluation. The chapter also includes the determination and analysis of structural velocity and frequency.

- Chapter four represents the results and detailed discussion and analysis of the results obtained from the prediction process.
- Chapter five concludes the research work.

CHAPTER TWO

LITERATURE REVIEW

Multiphase flow has been defined as the simultaneous flow of a mixture containing two or more phases or components. While there are a number of combinations of phases including liquid/liquid, liquid/solid, gas/solid and gas/liquid, gas/liquid flow is the most commonly encountered type of two phase flow (Anumbe & Khan, 2018). The study of multiphase flow is very important in energy-related industries and applications.

2.1. Important Parameters in Two Phase Flow

The knowledge of how to correctly evaluate the key variables of fluid mixtures and variables of individual phases or components is important to be able to effectively analyze the concept of two phase flow. The decision of whether or not to characterize the properties of the mixture and of its gross variables as averages or a sum of the partial properties and variables of each phase or component is the subject two-phase flow properties and variables. Flow patterns in two phase flow also depend on these flow parameters. Some of the important two-phase flow properties and variables are discussed below:

Liquid hold up and Void fraction

Liquid holdup can be defined as the ratio of the space occupied by the liquid phase to the total space available for fluid flow. Gas holdup or void fraction on the other hand is the ratio of the space occupied by the gas phase to the total space available for flow. Since the density of the gas phase is not constant along a given tube length, this parameters varies along it. They can be determined by the following expression:

$$H_L = \frac{A_L}{A}$$
$$\alpha = \frac{A_G}{A}$$

Where H_L is the average liquid holdup, α is the void fraction, A_L is the area of the pipe occupied by the gas phase, A_G is the area of the pipe occupied by the liquid phase and A is the area of the pipe. The liquid holdup and void fraction should sum up to unity ($H_L + \alpha = 1$).

Determining the void fraction is a simple task when the two phases are flowing in a homogenous manner with no relative velocity. However, in almost all cases, the velocities are different giving rise to the 'slip' phenomenon. This complicates the void fraction calculation. Various methods which include the use of selected models and empirical correlations have been employed by researchers in past and present studies to correctly evaluate these parameters. Some of these studies and their findings are presented in the last section of this chapter.

Mass Flow Rate:

This is the rate at which the mass of fluid passes through a location per unit time. The mass flow rates of the two phases are usually accounted for in two phase flow. It is usually denoted by 'W'. W_L , W_G and W are the liquid mass flow rate, gas mass flow rate and total mass flow rate respectively. For two phase flow;

$$W = W_L + W_G$$

Mass Flux:

This is the mass flow rate per unit area. It is usually denoted by 'G'. The mass fluxes for the gas and liquid phases are denoted as G_L and G_G . The summation of the mass fluxes of the two phases adds up to the total mass flux of the mixture.

Volumetric flow rate

This is the rate at which the volume of a fluid passes through a channel per unit time. It is usually accounted for in two phase flow analysis. It is denoted by 'q'. Where q_L & q_G are the liquid and gas volumetric flow rates respectively.

HYT65

Superficial velocity:

This is the hypothetical flow velocity calculated as if the given phase or fluid is the only one flowing or present in a conduit of a given cross sectional area. It is given by:

$$u_s = \frac{Q}{A}$$

Where Q is the volumetric flowrate of the phase measured in m^3/s and A is the cross sectional area measured in m^2 . It is used many engineering equations because it is the value which is usually readily known and unambiguous, whereas real velocity is often variable from place to place.

Mixture velocity:

This is the total volumetric flow rate of both phases per unit area. It could also be defined as the sum of all the superficial velocities of all the phases.

Mathematically, this is given as:

$$v_M = \frac{q_L + q_G}{A} = u_{SL} + u_{SG}$$

Slip/No-Slip:

Slip in two phase flow system is the difference between the true velocity of the gas and liquid phase. It exists when the velocity of the two phases vary. Slip velocity or velocity ratio is a term used to describe the relative motion between different phases in a fluid mixture.

Mathematically, it is given as:

$$v_{slip} = v_G - v_L$$

The slip velocity is negative when the liquid flows faster than the gas. Negative values of slip velocity are experienced in downward flow condition. When the relative velocity between the two phases is zero, the flow is characterized as **No-slip**.

In developing the homogeneous model of two-phase flow, the slip ratio is assumed to be unity (no slip).

Density

Two-phase flow density is necessary for multiphase flow analysis. For example it is required for the solution of pressure gradient equations. Like many other two-phase fluid properties, it can be determined using an averaged equation:

$$\rho_M = \rho_L H_L + \rho_G (1 - H_L)$$

In the special case where there is a non-slip assumption, the density can be given as follows:

$$\rho_{M(No\ Slip)} = \rho_L \lambda_L + \rho_G \lambda_G$$

Viscosity:

The concept of viscosity in two-phase flow is rather vague, but is nonetheless required for the determination of several dimensionless numbers (Reynolds number in particular).

Though it is more accurately determined using laboratory data or empirical correlations, the equation below suffices in many two-phase flow situations.

$$\mu_M = \mu_L H_L + \mu_G (1 - H_L)$$

2.2. Flow Regimes

A flow regime can be defined as a description of the geometrical configuration or morphological arrangement of the phases within a conduit or pipe.

Over the years, researchers have tried to come up with names for flow regime or flow pattern identification. An understanding of phase distribution into flow regimes, its transition

from one flow pattern to another and how it affects a two-phase system is essential to accurately predict gas-liquid flow behaviour. This has been a major area of concern in the oil and gas industry and has been widely investigated by several studies.

Flow regimes can be divided into three main classes: horizontal flow regime, vertical flow regime and regimes for sloped pipes. Many of the pressure drop, heat transfer and void fraction correlations often depend on knowledge of the flow pattern for their correct use. Flow patterns almost always form a part of any two phase flow study. However, flow pattern recognition is subjective in nature and depends to a certain degree on the interpretation of the researcher. Most researchers agree on the basic flow patterns that exist. The observed flow patterns depend largely on the orientation of the tube/pipe. While some flow patterns are common to all inclinations, others are characteristic of a particular inclination. This literature review considers only horizontal co-current flow in pipes.

2.2.1. Regimes for Horizontal Flow Pipes

In this type of flow regime, the heavier phase (liquid phase) is situated at the bottom of the pipe as a result of gravity. Generally, the gas phase pushes the liquid phase along the flow direction. According to (Anumbe & Khan, 2018), the most common classifications of horizontal pipe flow regimes includes the Stratified Flow, Intermittent Flow, Annular Flow and Dispersed Bubble Flow.

Stratified Flow: In this type of flow, the two phases are totally separated with gas phase located at the upper of the pipe section and the liquid phase located at the lower part of the pipe. It is commonly encountered at low gas and liquid flowrates and relatively smooth surface. The flow is classified as stratified wavy flow when the interface between the gas and liquid is wavy and stratified smooth flow when the interface is smooth.

Intermittent flow: This flow pattern is encountered when the gas velocity is increased beyond the levels experienced in the stratified flow regime. When this happens, the waves become bigger and the continuous interface which divides the two phases is distorted and the fluid in the pipe becomes non-uniformly distributed around it. This non-uniformity is expressed by alternate flow of liquid and gas. The liquid slugs are intermittently separated by large gas pockets with a stratified liquid layer flowing along the bottom of the pipe. While some studies like (Dukler, 1986) classified this flow pattern into it into slug, plug and elongated flow, others have classified it into only two categories (plug and Slug flow) only. Plug flow is identified by its distinct gas-liquid boundaries with its elongated bubbles moving at the same velocity as the liquid. The liquid slug is free of small bubbles. As the velocity of the gas phase increases, the magnitude of the wave increases and Slug flow emerges. Liquid slugs are formed as a result of the continuous buildup of the waves which eventually reaches the upper wall of the tube.

Annular Flow: In this type of flow, gas flows in the middle of the pipe with liquid droplets travelling along it. A coat is formed around the walls of the pipe by the liquid phase. Due to the effect of gravity, the coat formed tends to be thicker at the bottom than at the top.

Dispersed bubble flow: This type of flow is characterized as the flow where one phase is dispersed in the other continuous phase. It is observed at very high liquid flow rates with the gas phase distributed as discrete bubbles within a continuous liquid phase. Most of the bubbles are situated close to the upper pipe wall at the transition boundary. The bubbles are further separated uniformly along the entire regions of the pipe as the liquid flow rate is further increased.

This type of flow is considered homogenous no-slip since the two phases move at the same velocity with no slip between them.

The figure 2.1 below shows the different types of flow regimes observed for horizontal flow in pipes;

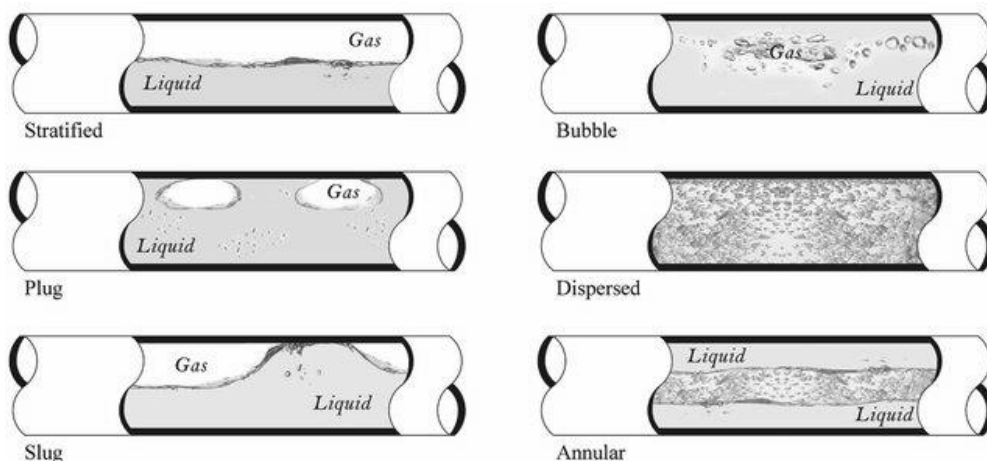


Figure 2.1-Flow Regimes for Horizontal Flow in Pipes

2.2.2. Regimes for Vertical Flow in Pipes

In this type of flow regime, the liquid phase tends to be on the pipe walls, forming a stable or an unstable film. Flow velocity could vary and different flow patterns could be encountered for upward and downward flow in pipe.

Among the major flow patterns that has been reported by many researchers for this flow regime type includes the bubbly, slug, churn, and annular flow.

Bubbly Flow: This type of flow regime is common at low gas flowrate. The gas phase is uniformly distributed and forms small discrete bubbles in a continuum of liquid. The bubbles size and shape could vary, though small sized and spherical shaped bubbles are the most

encountered. It occurs at relatively low liquid flowrate with low turbulence and slippage between the gas and liquid phases.

Slug Flow: As the gas flowrate increases, the bubbles draw closer to one another. Collisions between bubbles occur and eventually the bubbles start to coalesce, large bullet shaped bubbles known as Taylor bubbles are formed when they coalesce. Tiny spaces filled with a liquid film exist between the Taylor bubble and the pipe wall. Successive Taylor bubbles are separated by slugs of continuous liquid that contain small gas bubbles. Slug flow is found to be symmetric in vertical circular pipes,

Churn Flow: This is the type of flow pattern observed when the gas flowrate is increased beyond the rates in slug flow. When this happens, the concentration of the gas phase in the slug that exists between the successive Taylor bubbles is destroyed leading to a failure of the liquid slugs.

Almost simultaneously, the Taylor bubbles (in the slug flow) begin to respond to the failure of the liquid slugs and unrelated increase in gas concentration by breaking up into unstable patterns which are more chaotic, disordered and frothy than slug flow. The flow that finally emerges comprises of large shaped bubbles which are irregular in shape with smaller bubbles entrained in the liquid phase. This flow is said to be intermittent with liquid and gas mixing, churning together, fluctuating up and down in the channel and producing density waves. Any further increases in the gas flow rate would now give rise to a flow pattern that is even more disordered. This flow pattern is recognized by some researchers as froth flow.

Annular Flow: Annular flow develops from churn flow when the gas flow rate is increased. In this case, the bubbles formed coalesce into larger ones thereby occupying the entire diameter of the pipe with the liquid film flowing along the walls of the pipe.

Under certain conditions, the gas bubbles can become entrained within the film. At high liquid flow rates, the liquid droplets become concentrated and coalesce into wisps. This is identified as a wispy annular flow.

Dispersed bubble flow: In this type of flow, most of the cross-sectional area of the pipes the gas-phase is occupied by dispersed discrete bubbles in a continuous liquid-phase.

The figure 2.2 below shows the different types of flow regimes observed for vertical flow in pipes;

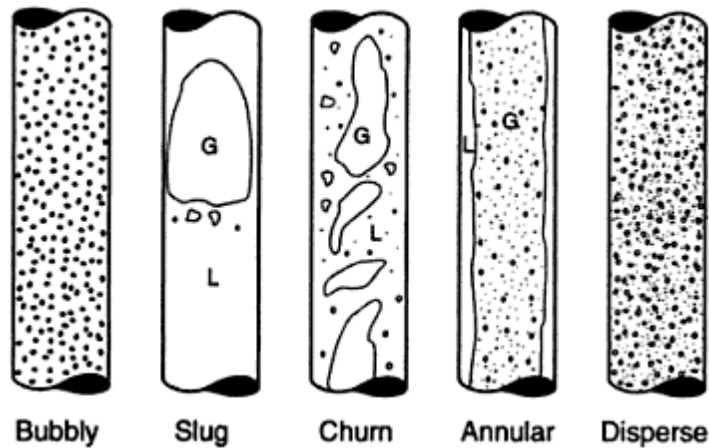


Figure 2.2- Flow Regimes for Vertical Flow in Pipes

For inclined flow pipes, the flow pattern in an inclined pipe is reportedly different from that of horizontal and vertical pipes. This is because when a pipe is inclined, the effect of gravity matters and alters the process of the fluid transport and the nature of the flow regimes.

2.3. Flow Pattern Identification Techniques

To easily identify the aforementioned flow regimes, several maps and correlations have been developed by different researchers. The easiest and simplest being the use of maps. To predict a particular flow pattern, the boundaries in which the flow pattern dominates is drawn and located knowing the mass flux, the liquid and gas superficial velocities. Flow pattern maps can be graphically categorized for both vertical and horizontal multiphase flows. Once all pattern boundaries observed are mapped, a clear overview of the behaviour can be observed as a function of flow conditions. There are two main types of techniques for identifying flow patterns. These are the theoretical and experimental flow pattern maps.

2.4. Flow Pattern Maps

A flow pattern map is a graphical representation of the occurrence of various flow patterns in the course of two phase flow. The axes of the map directly or indirectly represent the flow rates of the two phases. Transition lines or bands on the graph separate the different flow patterns visible at specific combinations of the flow rates or related quantities. The lines separating the flow patterns are regarded as zones and not a distinct line. This is because the change or transition of flow from one type to the other is a gradual process.

Flow pattern maps are generated with the aid of experimental data obtained from flow regime studies. Once the various flow regimes or patterns have been identified, the data obtained are plotted on a two dimensional plot to create the flow regime maps. The flow

regime maps are very vital tools which has been widely researched and applied in the field of two phase flow.

Flow patterns and flow maps are subject to differences in interpretations and experimental setups. While broad agreements exist between the results of researchers, specific differences are always present.

For creating two phase flow regime maps, two flow parameters (one for the ordinate axis and another for the abscissa axis) are usually required for creating the flow maps. These could be the combination either of the parameters such as the gas superficial velocity, liquid superficial velocity, gas mass flowrate, liquid mass flowrate and so on .

The application of flow pattern maps is limited within the range of conditions under which they were developed.

(Baker & Creager, 1954) provided one of the earliest and most widely used flow pattern maps for an air-water system. This superficial mass flux terms for the gas and liquid phases are used in this map.

Flow Pattern Maps for Horizontal Flow

(Mandhane et al., 1974) developed a map which has been applied in various horizontal two phase flow studies. Most of the maps developed later often compare their findings with this map. Other maps include (Weisman & Kang, 1981) and (Theofanous & Hanratty, 2003).

The flow patterns discussed above all differ at least slightly from one another. This is attributed to the difference in the experimental setups used by different researchers and the parameters of the experiments.

(Taitel & Dukler, 1976) developed a theoretical model for the various flow pattern transitions. From the mathematical analysis of the physics involved in various transitions, five dimensionless parameters were realized.

2.5. Predictive Modelling

This is the process of using known results to generate, process and validate a model that can be used to forecast future outcomes (Frankenfield, 2019). It is a tool used in predictive analytics. Predictive analytics involves the use of statistics and modelling to estimate future performance based on present and past information (Halton, 2019). The use of predictive modelling tools mostly through computer software programs have been vastly applied in industries especially when dealing with data that are voluminous in nature and are usually unstructured and too complex to be analyzed by humans within a short period of time. These computer software programs process large amount of historical data, accesses them,

identify a trend within the data, and provide a historical record as well as assessment of what behaviours or events a high likelihood of occurring again has.

Predictive analytics applies the use of predictors or known features to create models that can be used in obtaining output (Halton, 2019). A predictive model operates by learning how different points of data connect with each other. Two of the most widely used predictive modelling techniques are regression and neural networks (Frankenfield, 2019).

Predictive models are used in neural networks such as machine learning and deep learning which are both fields of artificial intelligence. Similar to the human brain, neural networks are made up of a web of interconnected nodes in hierarchical levels and stands as the basis of the artificial intelligence. Their ability to handle nonlinear data relationships and conquer the task of developing patterns between variables that would have proved impossible, too tedious or time consuming for human analysts to develop makes them stand out as a predictive modelling technique. The two basic types of predictive modeling techniques are discussed below:

Regression

This is a statistical method used to determine the strength and behavior of the relationship between a dependent variable and another or a series of other variables known as the independent variables (Beers & Westfall, 2020). It is used in the industries (mainly finance) to understand the relationships between variables. The two main types of regression are the simple linear regression and the multiple linear regression.

In the simple linear regression method, an independent variable is used to predict the outcome of a dependent variable Y. In the multiple linear regression method, two or more independent variable is used to predict outcome of a dependent variable. The two types of regression can be expressed as:

$$Y = a + bX + u$$

For simple linear regression, and

$$Y = a + b_1X_1 + b_2X_2 \dots b_tX_t + u$$

For multiple linear regression

Where:

Y=the variable that you are trying to predict (dependent variable)

X=the variable that you are using to predict Y (independent variable)

a=the intercept

b=the slope

u=the regression residual

Generally, regression takes a group of random variables, though to be predicting Y and tries to find a relationship between them. The relationship which is in form of a straight line gives the best estimate of all the individual data points.

Other predictive modelling techniques used to predict future outcomes include decision trees and Bayesian analysis.

Artificial Neural Network (ANN)

In its simplest form, an artificial neural network (ANN) is an imitation of the human brain (Harvey & Harvey, 1998). A neural network is a series of algorithms that strives to identify underlying relationships in a set of data via a process similar to the way the brain works. Naturally, the brain has the ability to learn new things, adapt to new and changing environment. The brain is also capable of analyzing incomplete and unclear information and makes its own judgment out of it. An artificial neural network consists of processing units called neurons.

The interest in models of neuronal networks or artificial neural networks generally arises from their ability to conduct interesting computational tasks (Vrahatis et al., 2001).

An artificial neuron tries to replicate the structure and behaviour of the natural neuron. A neuron consists of inputs (dendrites), and one output (synapse via axon).

The neuron has a function that determines the activation of the neuron. An illustration of a typical brain neuron and a model of an artificial neuron are shown in the figures 2.3 and 2.4 below:

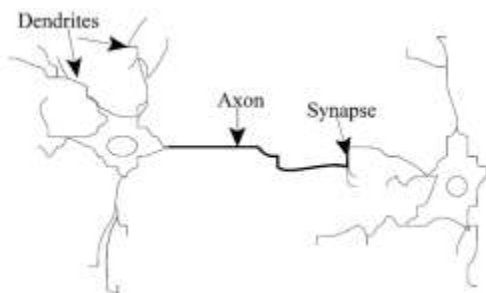


Figure 2.3: Brain neuron (Gershenson, 2003)

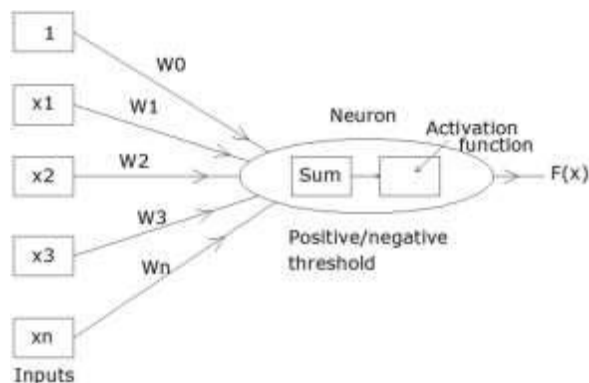


Fig 2.4: Model of an artificial neuron (Kuldeep & Anitha, 2017)

Where x_1, x_2, \dots, x_n represent the inputs to the neuron. w_0, \dots, w_n are the weights. A weight is the connection to the signal.

A bias is usually added to the neuron along with inputs. The addition of the bias is to introduce non-linearity into the transmitted signal. The value of the bias is initialized to 1. If the bias is not added, a linear function would result from the neuron and it would be limited to modelling only simple or easy data. It wouldn't be able to model complex data (Inzaugarat, 2018). Product of weight and input gives the strength of the signal. A neuron receives multiple inputs from different sources, and has a single output.

2.6. Activation Function

The Activation Function of a neuron determines if the neuron will be "fired" or not. In detailed terms; if the neuron would pass on a signal. This occurs via a calculation of the weighted sum and adding some bias to the result.

There are various functions used for activation. This includes the sigmoid function, threshold function, step function, linear function, ramp function, hyperbolic tangent function and the rectified linear units. Some of these functions are discussed below:

- **Sigmoid function**

The most commonly used activation function is the sigmoid function. It is a continuous and differentiable approximation of a step function. It is given by:

$$F(x) = \frac{1}{1 + e^{-sum}}$$

Where the sum is the weighted sum of the inputs multiplied by the weights between one layer and the next

$$sum = \sum_{i=0}^n x_i W_i$$

The limits of the sigmoid function range from 0 to 1. A graphical representation of the sigmoid function is presented in the figure below;

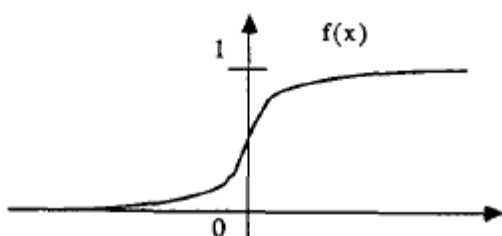


Fig 3: Sigmoid function

- **Threshold Function**

For this type of activation function, the decision on whether to transmit a signal is dependent on a certain threshold. The neuron is “fired” and outputs the exact signal to the next layer if the input signal is above a threshold (Luhaniwal, 2019)

- ***Hyperbolic tangent (tanh) function***

This is similar in shape to sigmoid, but its limits are from -1 to +1.

- ***Rectified Linear Units***

This is the most efficient activation function, ranging from 0 to infinity. This function is only applied to hidden layers, while outputs could utilize other functions (Luhaniwal, 2019).

2.7. ANN Architecture

The ANN architecture comprises of three basic layers:

- Input layer: which receives the input values
- Hidden layer(s): A set of neurons between input and output layers. There can be single or multiple layers
- Output layer: Usually it has one neuron, and its output ranges between 0 and 1, that is, greater than 0 and less than 1. But multiple outputs can also be present (Shukla & Abdelrahman, 2004).

The simplest form of ANN architecture is the Perception; this consists of a neuron with two inputs and one output. They are used for classification of data into two separate classes. The activation function used is step function or ramp function. For more complex applications, multilayer perceptions (MLP) are used, which contain one input layer, one output layer, and one or more hidden layers as given.

2.8. Methods of Adjusting Weights

The processing ability is stored in inter-unit connection strengths, called weights (Kuldeep & Anitha, 2017). Input strength depends on the weight value. Weight value can be positive, negative or zero. Negative weight means that the signal is reduced or inhibited. Zero weight means that there is no connection between the two neurons. The weights are adjusted to obtain the required output. There are algorithms to adjust the weights of ANN to get the required output. This includes the Brute force, the batch and stochastic gradient descent methods as discussed below:

- ***Batch-Gradient Descent***

This is a first-order algorithm which iterates through the data using various angles of the function line. It goes down the curve for a negative slope and upwards for a positive slope. It is only effective, for a convex-shaped curve (Mayo, 2017).

- ***Brute-force Method***

This is highly efficient or optimal when it is applied in a single-layer feed-forward network. After the other weights have been eliminated, the optimal weight is selected. The most minimal weight (the weight situated at the bottom of the curve) is the optimal weight. This method is easily affected by dimensionality (Mayo, 2017).

- **Stochastic Gradient Descent**

In this method of adjusting weights, a part of the original sample is picked randomly rather than iterating through the entire data as is the case in the Batch-gradient Descent. For non-convex shaped curves, the Stochastic Gradient is used instead. It is faster than the Batch-Gradient Descent (Mayo, 2017).

This process of adjusting weights is called learning or training (Gershenson, 2003).

Based on learning methods, ANN can be classified into supervised and unsupervised learning methods.

In Supervised learning method, training data contains key information, from which new information could also be found for “test examples”. In this case, the environment is the teacher that guides the learner towards the required information (labels) (Ben-David et al 2014).

In Unsupervised learning method, a difference between the training data and test data is not needed. The learner is fed the entire dataset and it then clusters the various groups of data, based on similarities between them (Ben-David et al 2014).

2.9. Ann Training Process

The process of giving a neural network known input data and asking it to obtain a known output is referred to as ‘training the network’ (Harvey & Harvey, 1998)(Purvis & Kuzma, 2016). The network is said to be trained after it has undergone many **epochs** (the cycle of going forward from input and output, and from output to input) till the error is within a certain tolerance. An error is the difference between actual output and desired output. This process of training sets the weights between all the neurons in all the layers. The weights so obtained from a trained network are used in calculating the response of the network to an unknown data.

More knowledge is acquired about the features of the data during this process. The model also classifies the output for each input in the training process. After this classification occurs, the loss will then be calculated, and the weights in the model will be adjusted. Then, during the next epoch, it will classify the same input again.

The most common method of training the neural network is the Back propagation algorithm. In this case, the difference between a targeted output and the output obtained is propagated back to the layers and the weights are adjusted. A back propagation neural network (BPNN)

uses a supervised learning method and feed-forward architecture. It is one of the most frequently applied neural network techniques for classification and prediction.

2.10. ANN Validation Process

Just as the model is trained on the training set, the model will also be validated on the validation set. This validation process helps give information that may be useful in adjusting hyper parameters. In this process, a set of data, separate from the training set, is used to validate our model during training.

The model classifies each input from the validation set. This classification is based only what it has learnt about the data during the training process. Unlike the training process, the weights are not adjusted in the model based on the loss calculated from the validation data after classification.

The main aim a validation set is needed is to ensure that our model is not overfitting to the data in the training set. The validation set allows us to see how well the model is generalizing during training.

Overfitting occurs when the model becomes really good at being able to classify data in the training set, but it's incapable of generalizing and making accurate classifications on data that it wasn't trained on. Provided the results being obtained from the model for the validation data is just as good as that obtained during the training process, the model can be said to be free from overfitting.

However, if the results from the training process are good, but that from the validation data are lagging behind, then the model is overfitting.

2.11. ANN Testing Process

After the model has been trained and validated using the training and validation sets, it is then used to predict the output of unlabeled data in a test set.

The test set is a set of data that is used to test the model after the model it has been previously trained. It is different from both the training set and validation set.

The test set is different from the training and validation set as it is usually not labeled. The training set and validation set have to be labeled so that we can see the metrics given during training, like the loss and the accuracy from each epoch.

If the model can successfully predict unlabeled data in the test set, then the process can now be applied into the field.

Advantages of Ann

ANN is different from a normal computer program in many ways. Some of its features include:

- ANN is quite fast as compared to brain processing time which is slower
- Its ability to learn how to do tasks while learning just like the human brain does.
- Its ability to create its own organization while learning. This is not the same with a normal program that is fixed for certain task and won't do any other thing than what it is intended to do.
- ANN carries out its operations in parallel like a human brain unlike other computer program which works serially.
- Unlike a normal program, ANN can still work even when the data provided is incomplete, noisy, or ambiguous.

Limitations of Ann

The basic limitation of artificial neural network when compared with a normal computer program remains the fact the ambiguous (unclear) manner in which it calculates output. Though similar, the time taken to execute a task is not constant as it keeps changing with different sets of inputs

2.12. Review of Past Work on the Prediction of Liquid Holdup in a Horizontal Pipe

Several studies have been done in the past to analyze or characterize the concept of gas-liquid flow in a horizontal pipe. This include the identification of flow regimes, the analysis and prediction of pressure drop, liquid hold up and bubble velocity. This section of this chapter presents a review on the various works that has been conducted on the prediction of liquid holdup and other key parameters in gas-liquid flow with a focus mainly on horizontal pipe.

(Bagci & Al-Shareef, 2003) applied the use of a mathematical model and computer program to describe slug flow in pipelines (horizontal and inclined). Designed on the basis of the sink/source concept at the pipeline connections, this model was used to evaluate the liquid

holdup in horizontal and inclined pipes. Other models were also applied to evaluate the other parameters needed to perform the sink/source model. The film liquid holdup was observed to decrease with increase in pipe diameter. Unit slug length also increased at the upstream inclined pipe and decreased at the downstream inclined pipe with increasing pipe diameter. Slug characteristics were found to be mainly affected by low superficial gas and liquid velocities, large pipe diameters and shallow pipeline inclinations.

(Granados-C. & Camacho-V., 1998) developed a computer program for simulating two phase flow in horizontal and inclined pipes. The program based on the mechanistic model of Xiao et al. and it extended the range of angle of inclination from 15 degrees to 45 degrees with the help of the work carried out by Barnea and Hassan and Kabir. The program was used to determine key concepts such as flow patterns under stationary conditions, liquid holdup and pressure gradients in horizontal and inclined pipes. Model was compared to that of Beggs and Brill and similar trends were observed. It was also accessed using statistical parameters. The performance of the principal hydrodynamic parameters was also presented using 3-D graphs in this study

In the study carried out by (Al-Safran, 2009), a new correlation was developed for predicting slug liquid holdup in a horizontal pipe. This correlation was generated with the aid of a large data set with wide ranges of operational, geometrical, and physical property parameters. Findings in this study revealed that the dimensionless momentum transfer rate as an independent parameter accounted for a large part of the variation observed in slug liquid holdup. The accuracy of the new correlation was also validated through statistical evaluation. An average (in percentage) relative error and standard deviation of 4.1% and 2.4% were obtained respectively. The correlation generated was compared with other correlations and gave the best result among others with the lowest relative performance factor of 0.01.

(Shippen & Scott, 2004) developed neural network models with the aid of data obtained from five independent studies. While one of the models is based on discrete parameters including flow rates, pipe diameter, and fluid properties, the other model applied dimensionless numbers to incorporate these parameters. The developed models were compared with existing empirical correlations (Beggs-Brill, Minami-Brill, Mukherjee-Brill, Abdul) and mechanistic models (Taitel-Dukler, Xiao). It was observed that the performance of both neural network models developed were more consistent and accurate over a wide range of liquid holdup and flow patterns considered. Also, unlike the other approaches, the models do not require identification of flow pattern before they are applied and are therefore not affected by errors emanating from the prediction of flow patterns. The models were also

observed to be more capable of being applied to a wider range of flow conditions with the introduction of additional training data.

A study carried out by (Xiao et al., 2020) proposed a method for predicting the liquid holdup in horizontal pipe with BP neural network algorithm. This method was compared with empirical correlations for predicting liquid holdup; results obtained showed that the BP neural network model was more accurate with the smallest standard deviation of 8.65% and an average relative error of 7.38%. a sensitivity analysis on the key factors affecting liquid holdup was also carried out, results obtained showed that liquid and gas superficial velocities, pipe diameter and temperature are the key parameters influencing liquid hold up in a horizontal pipe. While the pipe diameter, liquid-phase superficial velocity, temperature, and viscosity are positively correlated with the liquid holdup, the pressure and gas-phase superficial velocity are negatively correlated with it.

CHAPTER THREE

METHODOLOGY

3.1. Data Acquisition

The liquid holdup data was obtained from the Multiphase Flow Research Group, Chemical and Environmental Engineering Department, the University of Nottingham, United Kingdom. The liquid holdup over a period of 12,000 time points (0s to 5995s) was recorded for an air–silicone oil system. This was done for planes 1 and 2 of the horizontal pipe setting. 13 different gas superficial velocities were varied (0.05-4.73 m/s) while the liquid superficial velocity (0.05-0.14 m/s) was kept constant for every liquid superficial velocity.

3.2. Data Processing

The raw data obtained from planes 1 and 2 was of key interest in this study. The time series raw data was processed to obtain the void fraction for different experimental runs. 39 different sheets corresponding to each gas superficial velocity varied for each plane were created, plots of void fraction against time and corresponding PDF plots were made for all the runs for both planes.

3.3. Predictive Model Selection

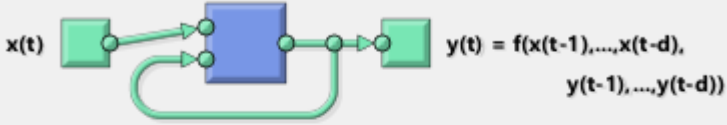
Due to its ability to predict non-linear data and high efficiency with time series data generally, the Artificial Neural Network (ANN) was selected as the preferred method for prediction. MATLAB has a Neural Network toolbox (ntstool) for time series data.

In this tool used for future prediction of time series data, there are three kinds of non-linear series problem. Out of the three choices, the “Nonlinear Autoregressive with External (Exogenous) Input” solution was used in this study. It was selected as the preferred choice as it is the most accurate than the other two in learning how to predict time series data when supplied with its past values. The model relates current values of the time series to both the past values of the same time series and an externally determined series to obtain values of the series of interest. Figure 3.1 shows the selection process.

Select a Problem

Nonlinear Autoregressive with External (Exogenous) Input (NARX)

Predict series $y(t)$ given d past values of $y(t)$ and another series $x(t)$.



$y(t) = f(x(t-1), \dots, x(t-d), y(t-1), \dots, y(t-d))$

Nonlinear Autoregressive (NAR)

Predict series $y(t)$ given d past values of $y(t)$.

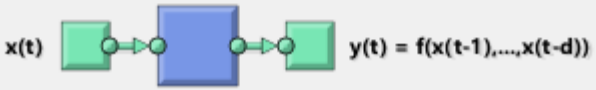


$y(t) = f(y(t-1), \dots, y(t-d))$

Nonlinear Input-Output

Predict series $y(t)$ given d past values of series $x(t)$.

Important Note: NARX solutions are more accurate than this solution. Only use this solution if past values of $y(t)$ will not be available when deployed.



$y(t) = f(x(t-1), \dots, x(t-d))$

Figure 3.1: Selecting the NARX as a solution to the time series problem

The log sigmoid transfer function was utilized as the transfer function in each of the hidden layers and the purelin transfer function was utilized for the output function.

3.4. Training of Neural Network

After selecting the predictive model to be applied, the time series data (values of liquid holdup and corresponding time intervals) for each of the runs was loaded onto the tool as showing in Figure 3.2:

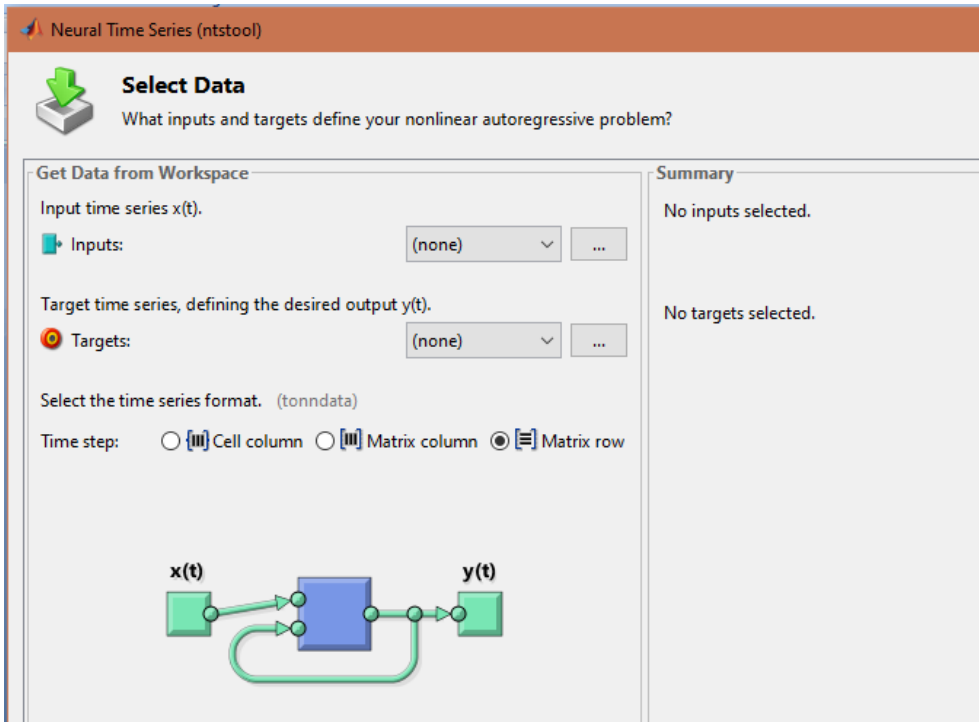


Figure 3.2-Importation of time series data

The input (corresponding time interval) and targets (liquid holdup) defines the non-linear autoregressive problem.

The 12,000 target sets of data were randomly divided for training, validation and testing respectively. As shown in Figure 3.3, 70% of the data set was allocated for training while 15% was set for both validation and testing.

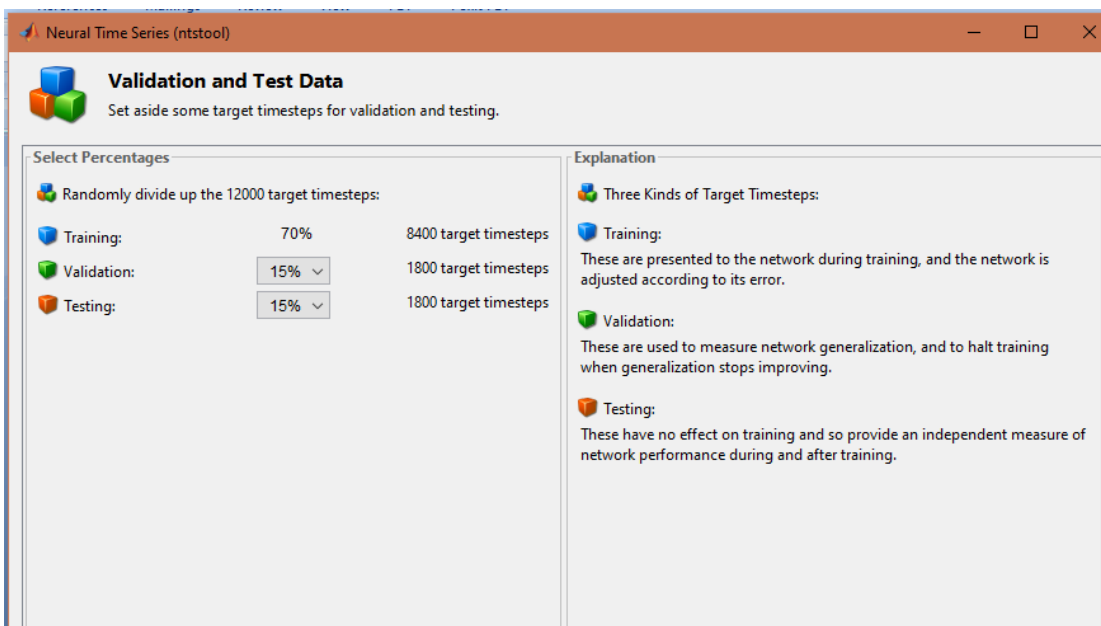


Figure 3.3-Splitting time series data set for training, validation and testing

Parameters required to run the simulation were defined. This includes the number of hidden neurons and the number of delays 'd'. A trial and error method is used to obtain appropriate number of hidden neurons and delays. As shown in Figure 3.4, the number of hidden layers was set at 10 for all runs. This was done after trying out different numbers. Any number exceeding 10 increases the training time and reduces computing speed. The number of delays was varied, until the best validation performance was obtain.

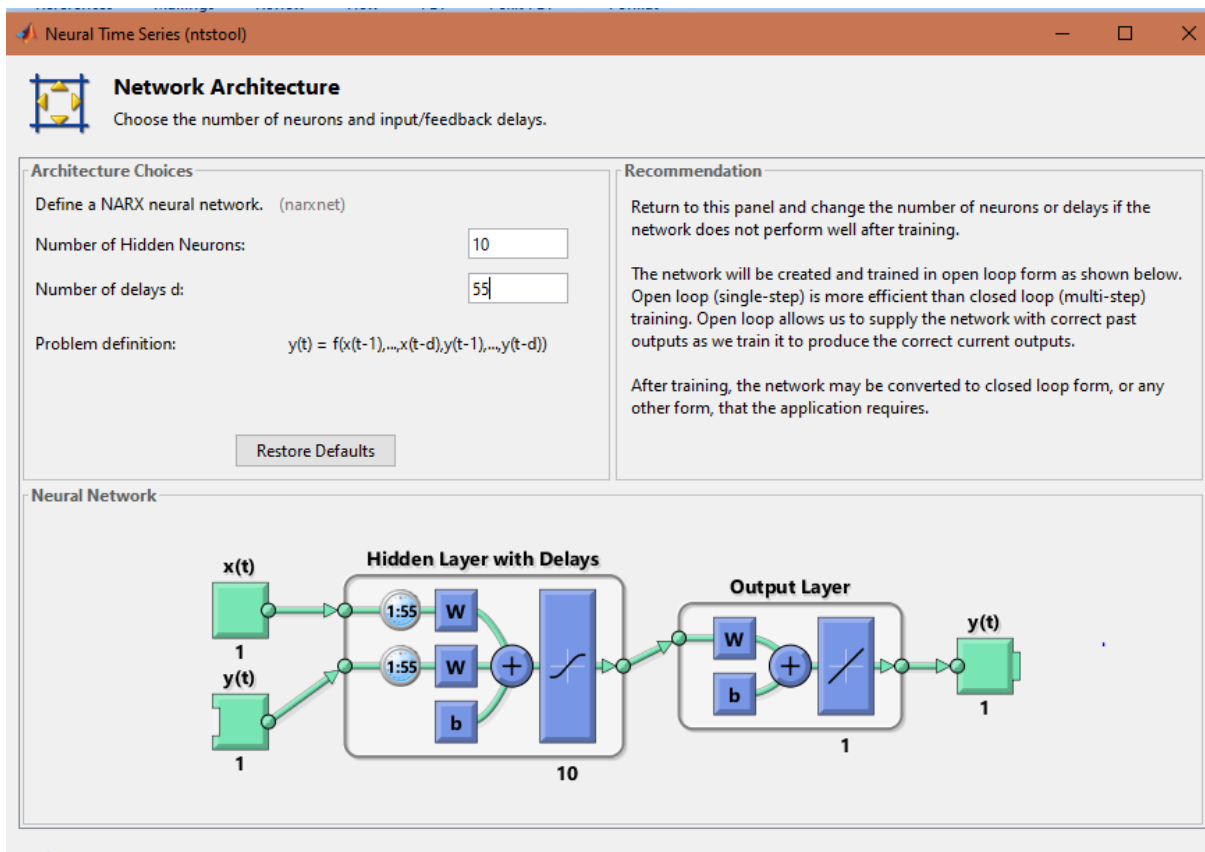


Figure 3.4-Architecture of Neural Network

Tables 3.1 and 3.2 show the neural network specification for both planes.

Runs	Liquid superficial velocity (U_{SL}), m/s	Gas superficial velocity (U_{SG}), m/s	Number of Hidden Neurons	Number of delay
1	0.05	0.05	10	50
2	0.05	0.06	10	50
3	0.05	0.29	10	50
4	0.05	0.34	10	80
5	0.05	0.4	10	70
6	0.05	0.54	10	70
7	0.05	0.71	10	80
8	0.05	0.95	10	95
9	0.05	1.42	10	81
10	0.05	1.89	10	55
11	0.05	2.36	10	70
12	0.05	2.84	10	95
13	0.05	4.73	10	95
14	0.09	0.05	10	95
15	0.09	0.06	10	95
16	0.09	0.29	10	100
17	0.09	0.34	10	90
18	0.09	0.4	10	90
19	0.09	0.54	10	95
20	0.09	0.71	10	95
21	0.09	0.95	10	95
22	0.09	1.42	10	100
23	0.09	1.89	10	100
24	0.09	2.36	10	80
25	0.09	2.84	10	80
26	0.09	4.73	10	88
27	0.14	0.05	10	90
28	0.14	0.06	10	95
29	0.14	0.29	10	97
30	0.14	0.34	10	89
31	0.14	0.4	10	90
32	0.14	0.54	10	92
33	0.14	0.71	10	98

34	0.14	0.95	10	100
35	0.14	1.42	10	100
36	0.14	1.89	10	93
37	0.14	2.36	10	100
38	0.14	2.84	10	93
39	0.14	4.73	10	100

Table 3.1- Neural Network Specification for each gas and liquid superficial velocity for plane

1

Runs	Liquid superficial velocity (U_{SL}), m/s	Gas superficial velocity (U_{SG}), m/s	Number of Hidden Neurons	Number of delay
1	0.05	0.05	10	50
2	0.05	0.06	10	50
3	0.05	0.29	10	55
4	0.05	0.34	10	55
5	0.05	0.4	10	58
6	0.05	0.54	10	60
7	0.05	0.71	10	65
8	0.05	0.95	10	65
9	0.05	1.42	10	65
10	0.05	1.89	10	89
11	0.05	2.36	10	92
12	0.05	2.84	10	78
13	0.05	4.73	10	83
14	0.09	0.05	10	86
15	0.09	0.06	10	89
16	0.09	0.29	10	91
17	0.09	0.34	10	92
18	0.09	0.4	10	92
19	0.09	0.54	10	93
20	0.09	0.71	10	91
21	0.09	0.95	10	95
22	0.09	1.42	10	89
23	0.09	1.89	10	90
24	0.09	2.36	10	94
25	0.09	2.84	10	94
26	0.09	4.73	10	95
27	0.14	0.05	10	95
28	0.14	0.06	10	95
29	0.14	0.29	10	95
30	0.14	0.34	10	98
31	0.14	0.4	10	98
32	0.14	0.54	10	96
33	0.14	0.71	10	96

34	0.14	0.95	10	96
35	0.14	1.42	10	92
36	0.14	1.89	10	100
37	0.14	2.36	10	100
38	0.14	2.84	10	93
39	0.14	4.73	10	96

Table 3.2- Neural Network Specification for each gas and liquid superficial velocity for plane 2

The next step is to select the appropriate training algorithm. Training algorithms exist to automatically adjust the bias and weights of the neural network. As shown in Figure 3.5, the Levenberg-Marquardt algorithm was used for training the network. It was selected because it requires less time when compared with the other training algorithms.

Training stops upon the increase in mean square error during validation performance evaluation.

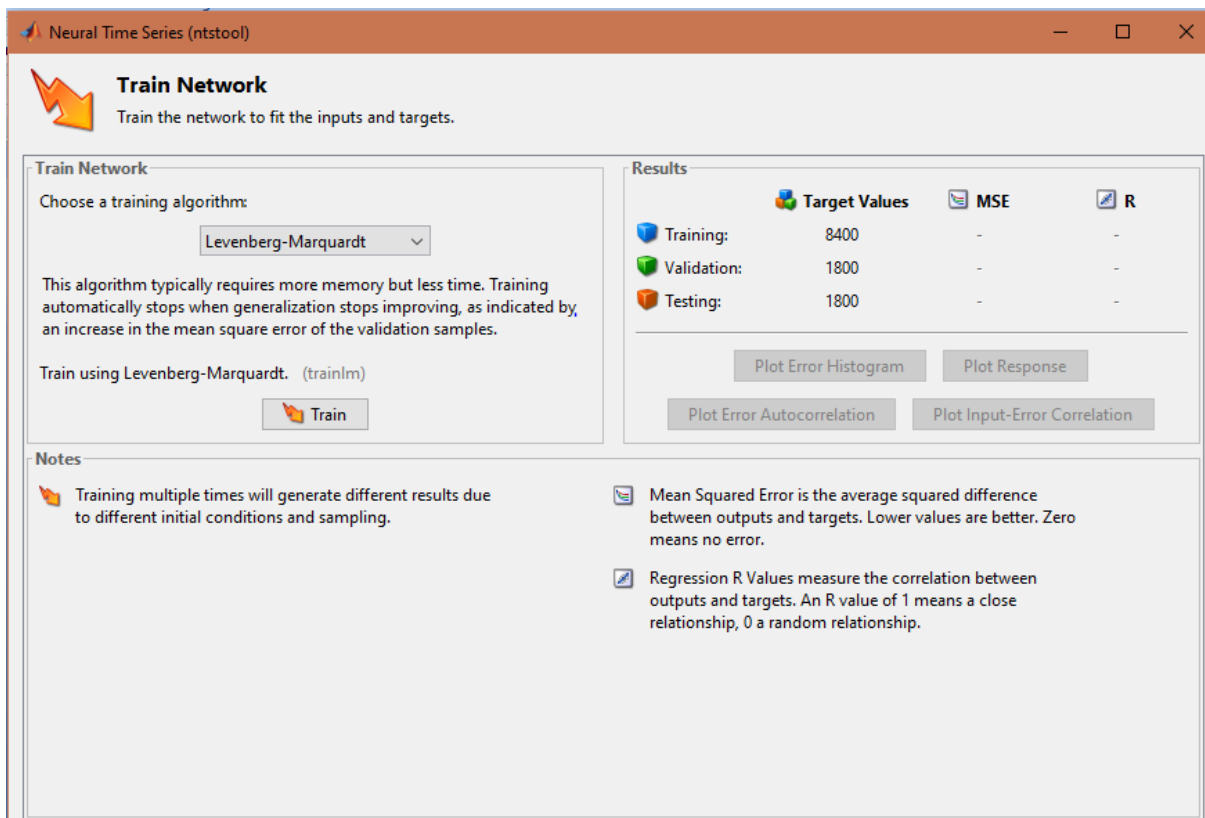


Figure 3.5- Training Algorithm Selection

Figure 3.6 shows the training process of the neural network. It could be seen that the training continued until the validation error failed to decrease for six iterations (validation stop).

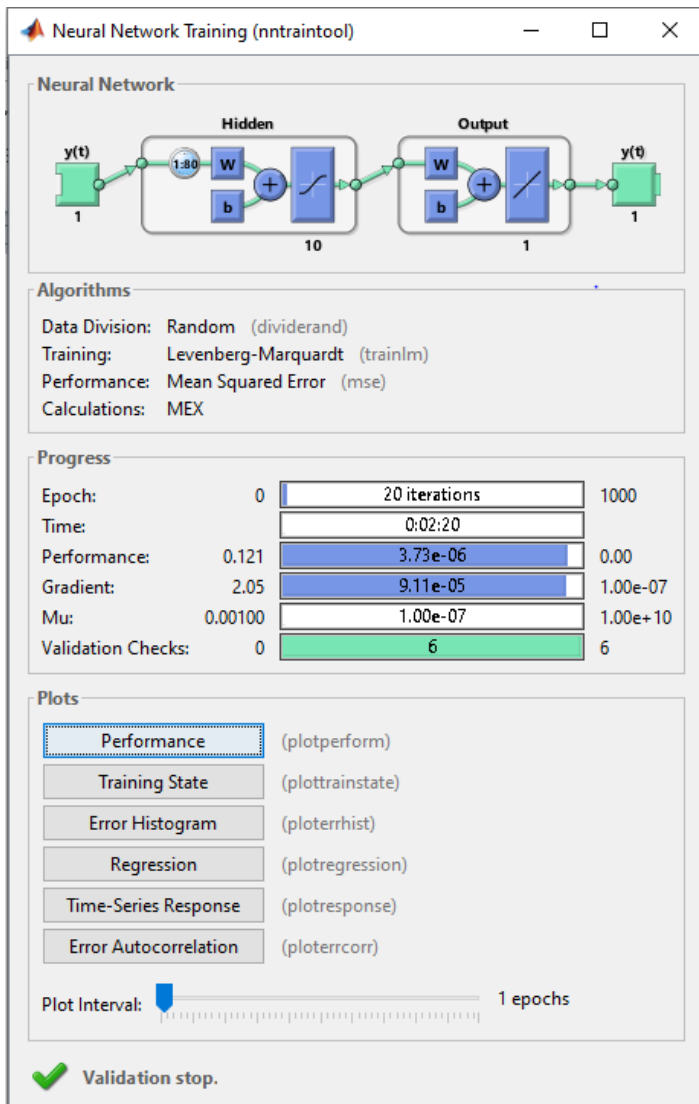


Figure 3.6- Training the neural network

3.5. Evaluating the Model

A neural network is the network which gives highly accurate result within the shortest possible training time. The efficiency of the neural network was monitored using the "Autocorrelation of Error 1 chart", where non-zero lags are within the confidence limit as shown in Figure 3.7.

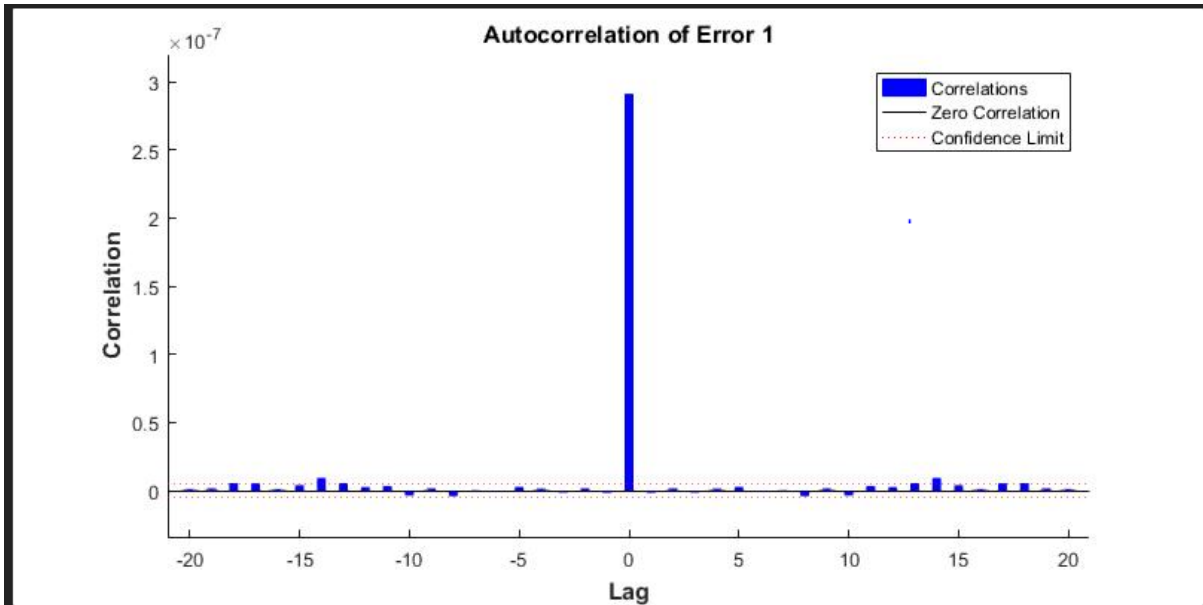


Figure 3.7-Autocorrelation of Error 1 chart

Other figures such as the time series response chart and the performance plots were also used to ascertain the efficiency of the neural network.

Experimental values from raw data and simulated values were placed in the same excel sheet(s). Average values of the liquid holdup for both experimental and simulated runs was evaluated and compared to ascertain the effective prediction ability of the ANN.

3.6. Determination of Structural Velocity and Frequency

The average liquid holdup data for planes 1 and 2 of each run were used in a MACRO cross correlation template to obtain the structural velocity after inserting the total number of data (12000), sampling frequency (200Hz) and distance between the sensors (0.089m). This was done for both experimental and simulated values.

Power spectral density (PSD) was run in macro after inserting the total number of data (12000) and sampling frequency (200Hz) to obtain the dominant frequency in each of the runs for both.

The effect of gas and liquid superficial velocities on the bubble velocity and slug frequency for the gathered experimental and simulated data was also investigated.

CHAPTER 4

4.0. RESULT AND DISCUSSION

In this section, an analysis of the neural networks efficiency in predicting time series data or liquid holdup was carried out using MATLAB charts and tables. The analysis was also carried out based on average liquid holdup, translational Taylor bubble velocity (structure velocity) and frequency obtained from the experimental data and the output from the prediction using MATLAB.

An analysis of the effect of increasing liquid and gas superficial velocities on bubble velocity and slug frequency was also carried out by plotting structural velocity and slug frequency against gas superficial velocity at constant liquid superficial velocity.

4.1. Analysis Based on MATLAB Charts and Tables

Three charts were used to analyze the results obtained from the neural network. These include the cross correlation and power spectral density (PSD) plots, and the time series performance response plot.

The error autocorrelation plots display the error autocorrelation function. It depicts the relationship between the prediction errors and time. It was used to validate the network performance. It is worth mentioning that for a perfect prediction model, there should only be one nonzero value of the autocorrelation function and it should occur at zero lag. All other lags should be within the confidence limit.

Fig 4.1-4.6 shows the error autocorrelation charts for planes 1 and 2. The figures represent a case study showing the MATLAB charts at a gas superficial velocity (U_{SG}) of 0.05 m/s and at varying liquid superficial velocities (U_{SL}) of 0.05 to 0.14 m/s for both planes.

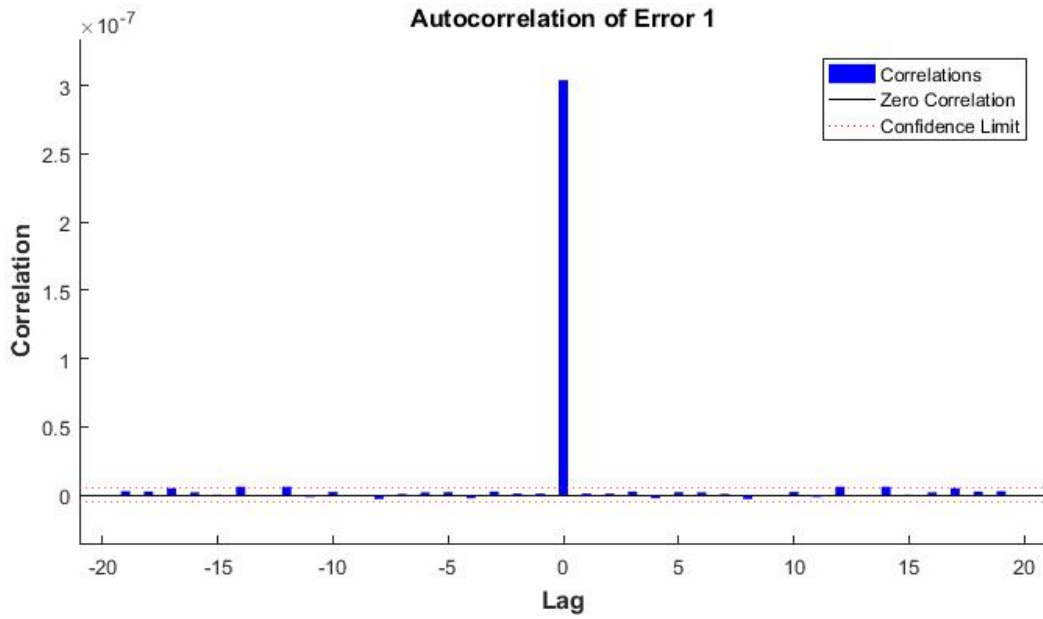


Figure 4.1- Autocorrelation of error 1 plot for plane 1 ($USL=0.05$ m/s, $USG=0.05$ m/s)

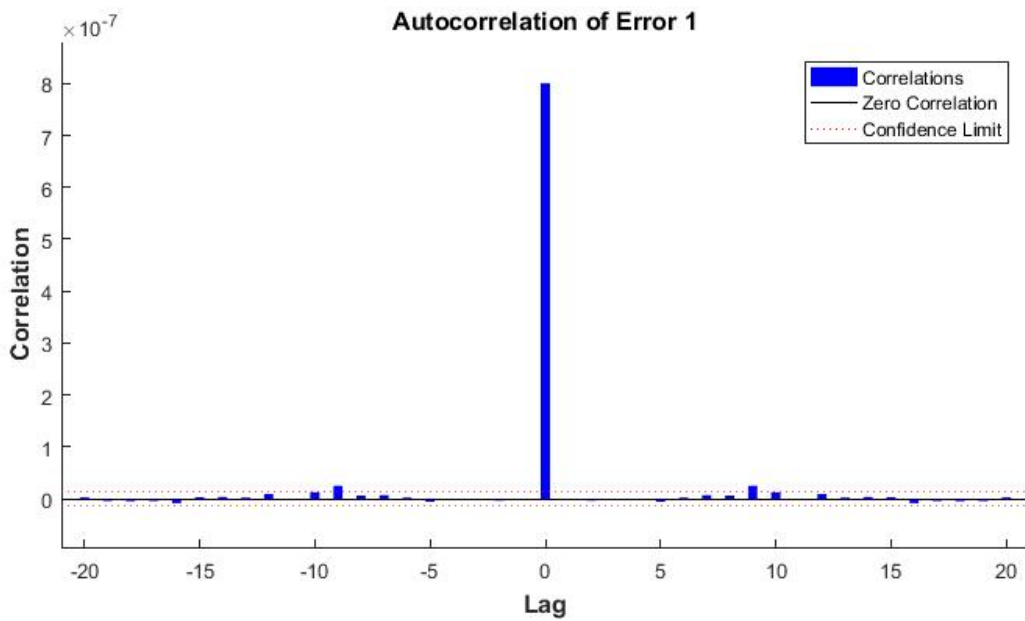


Figure 4.2- Autocorrelation of error 1 plot for plane 1 ($USL=0.09$ m/s, $USG=0.05$ m/s)

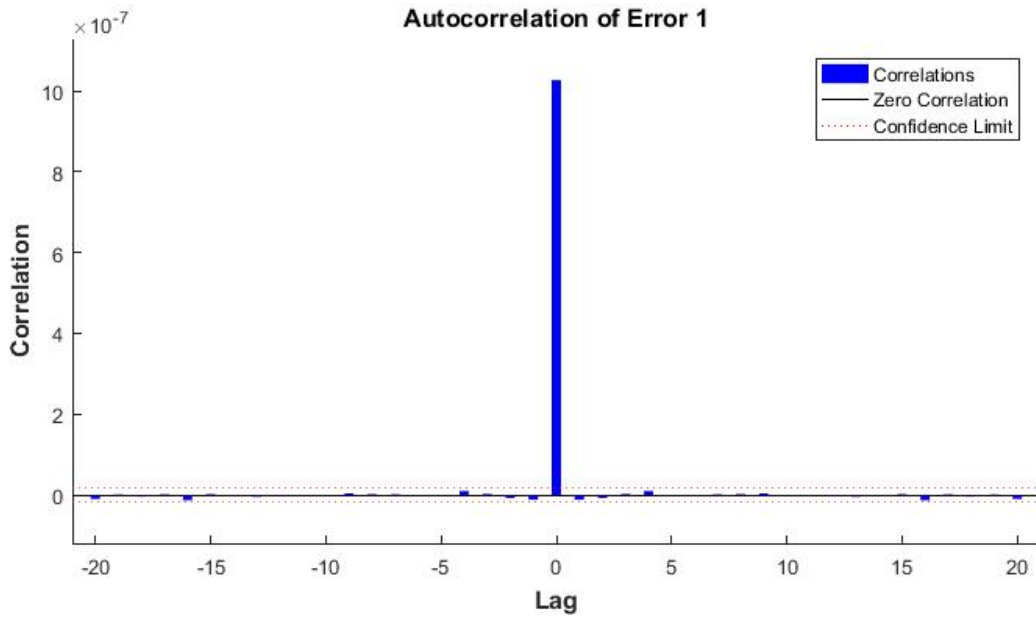


Figure 4.3- Autocorrelation of error 1 plot for plane 1 ($USL=0.14$ m/s, $USG=0.05$ m/s)

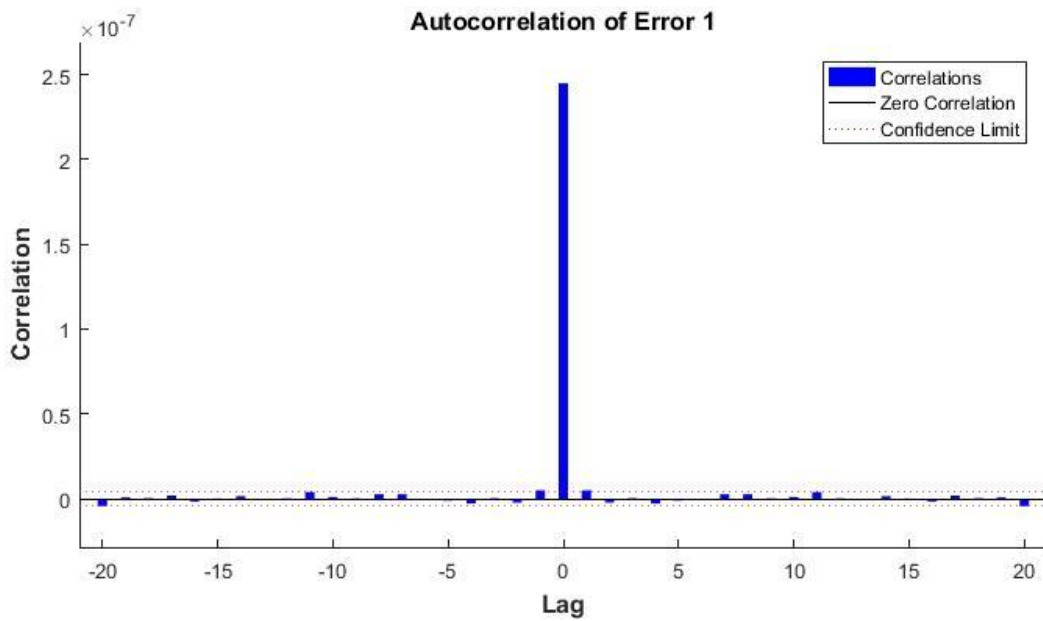


Figure 4.4- Autocorrelation of error 1 plot for plane 2 ($USL=0.05$ m/s, $USG=0.05$ m/s)

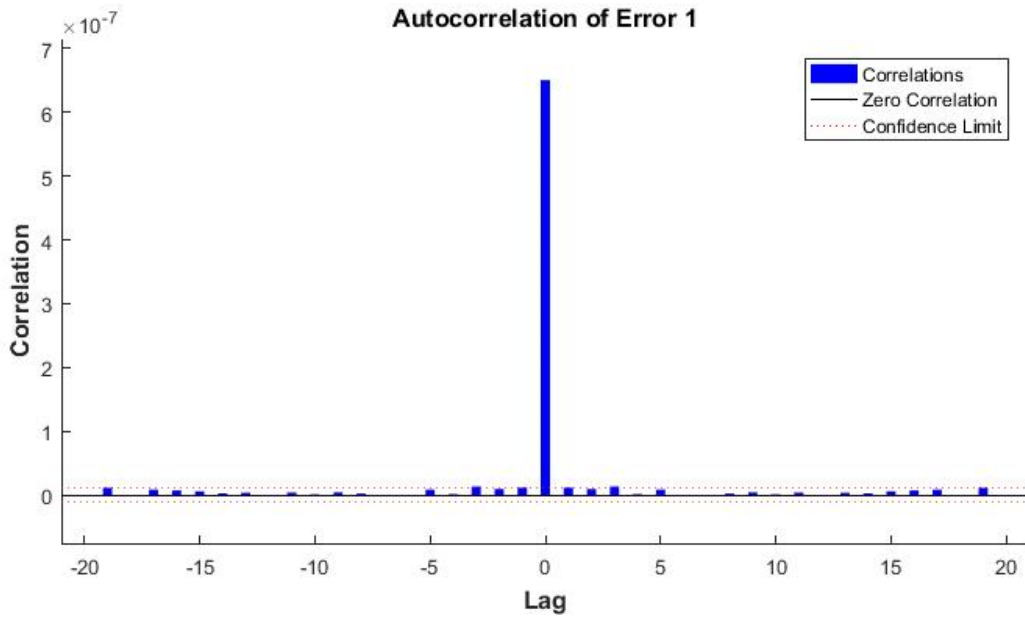


Fig 4.5- Autocorrelation of error 1 plot for plane 2 ($USL=0.09$ m/s, $USG=0.05$ m/s)

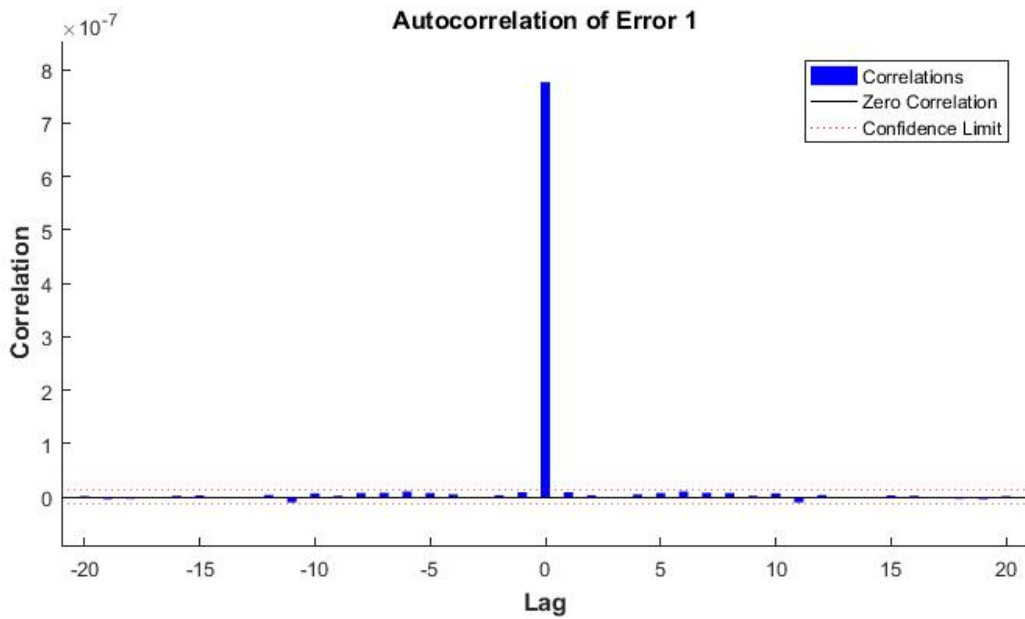


Figure 4.6- Auto correlation of error 1 plot of for plane 2 ($USL=0.14$ m/s, $USG=0.05$ m/s)

From the auto correlation of error 1 charts for all cases presented in the figures, it can be observed that besides from the error at the zero lag, error(s) at all other lags lie within the confidence limit. This therefore, depicts the efficiency of the neural network as a predictive model for this study.

Performance charts

The performance chart is a plot showing how the mean squared error (MSE) decreases with time during training, validation and testing. The number of iteration(s) at which the best performance of the neural network was obtained for each run is also obtained from this chart.

Figures 4.7-4.9 show the performance charts for plane 1. The figures, MATLAB charts depict a case study at a gas superficial velocities (USG) of 0.54 m/s at various liquid superficial velocities (USL) of 0.05 to 0.14 m/s for plane 1 is presented;

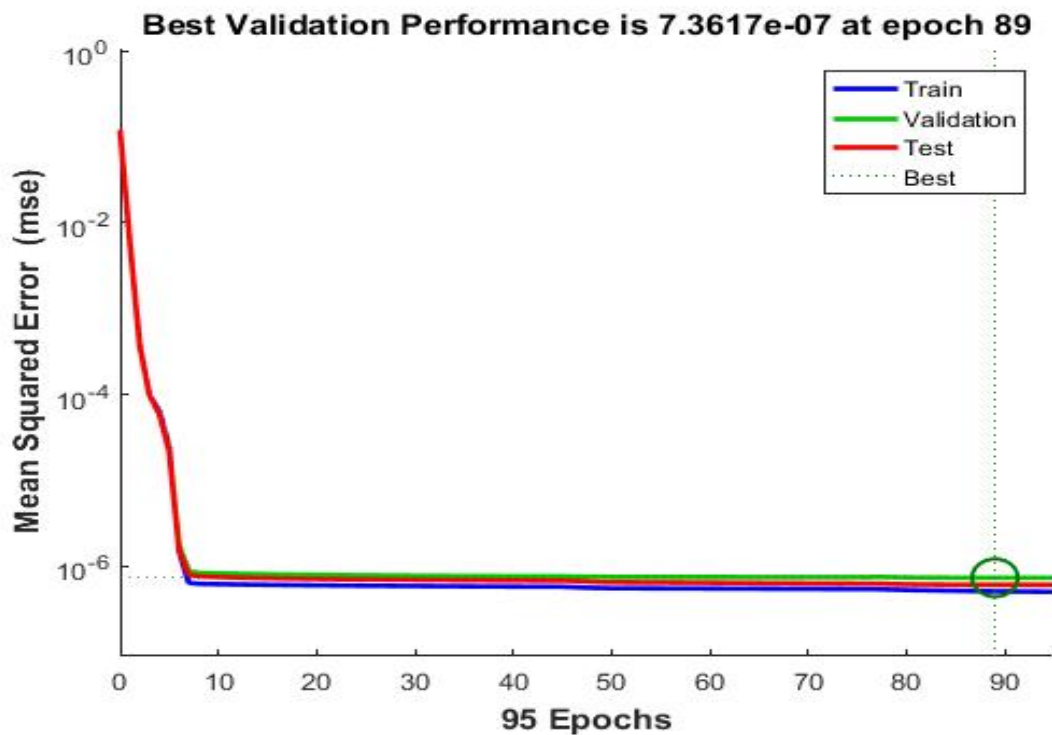


Figure 4.7- Performance plot for plane 1 (USL=0.05 m/s, USG=0.54 m/s)

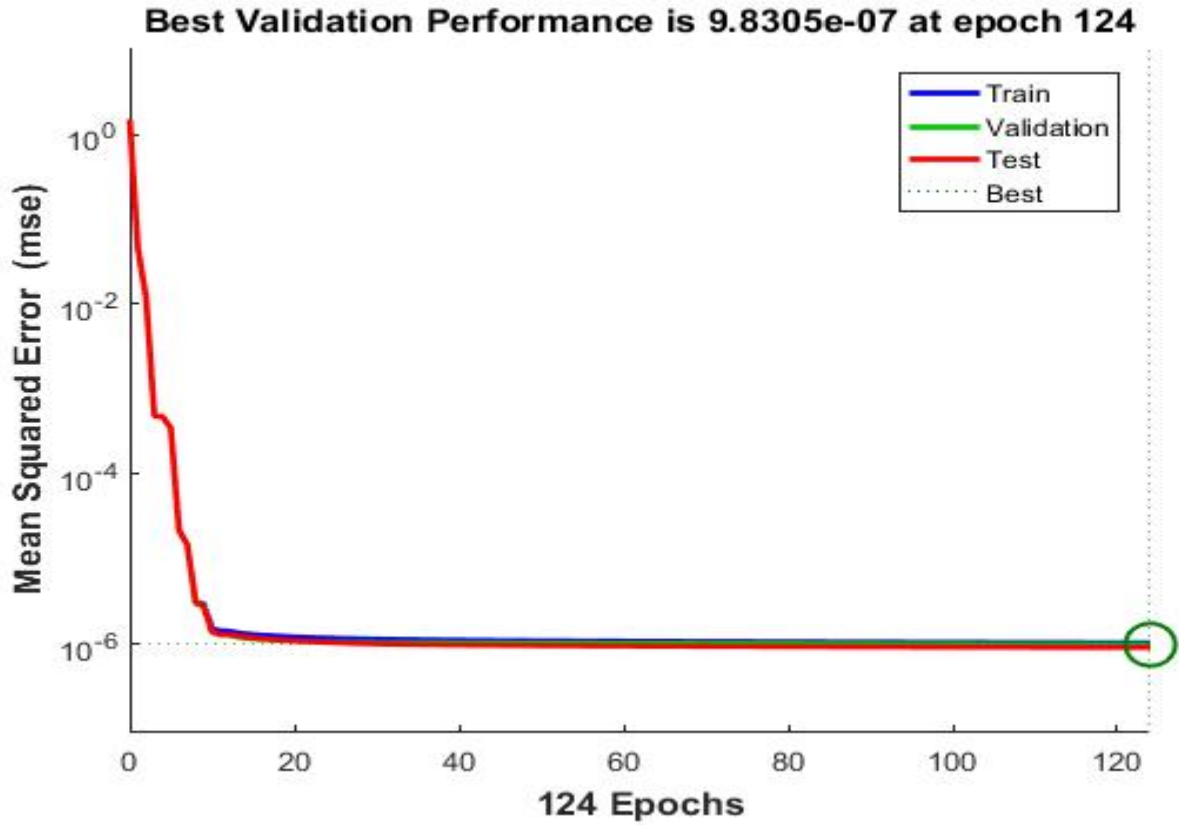


Figure 4.8- Performance plot for plane 1 ($USL=0.09$ m/s, $USG=0.54$ m/s)

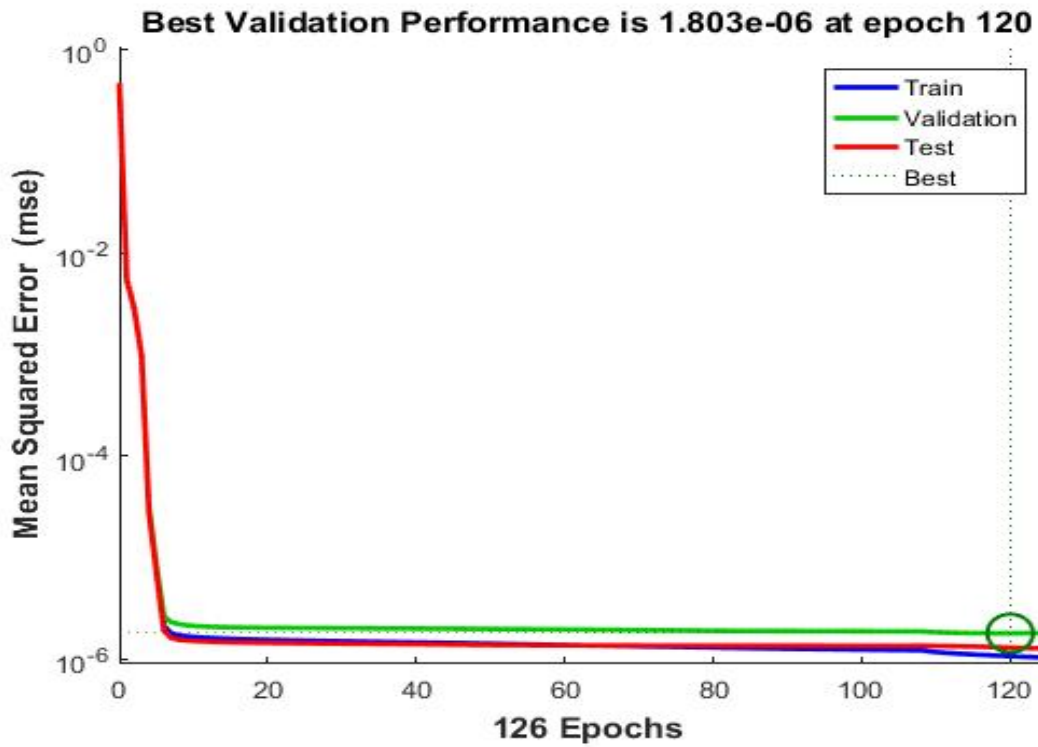


Figure 4.9- Performance plot for plane 1 ($USL=0.14$ m/s, $USG=0.54$ m/s)

A decreasing trend in the training and validation errors down till the highlighted epoch can be observed from the performance charts plotted in Figures 4.7 to 4.9. Also, overfitting does not seem to have occurred for the liquid and gas superficial velocities considered for both planes, as the validation error did not increase before the highlighted epoch.

Taking the liquid superficial velocity of 0.05 m/s, as a subject, the best validation performance was obtained at 89 epochs (number of iterations). In other words, the best performance was attained after the biases and weights were adjusted 89 times.

Tables 4.1-4.6 below shows the mean squared error (MSE) values obtained for the liquid and gas superficial velocities of planes 1 and 2 respectively. MSE values close to zero was obtained for all the runs in both planes. This further emphasizes the efficiency of the neural network in accurately predicting the liquid hold up.

Run	Gas Superficial Velocity, USG (m/s)	Epoch (Number of Iterations)	Mean Squared Error (MSE) values
1	0.05	64	5.123×10^{-7}
2	0.06	164	2.787×10^{-7}
3	0.29	170	2.145×10^{-7}
4	0.34	119	5.809×10^{-7}
5	0.4	328	4.655×10^{-7}
6	0.54	95	5.132×10^{-7}
7	0.71	64	5.609×10^{-7}
8	0.95	54	3.934×10^{-7}
9	1.42	177	4.193×10^{-7}
10	1.89	64	1.191×10^{-7}
11	2.36	24	1.359×10^{-6}
12	2.84	52	2.034×10^{-6}
13	4.73	14	4.616×10^{-7}

Table 4.1- Mean squared error (MSE) values for plane 1 (USL=0.05 m/s)

Run	Gas Superficial Velocity, USG (m/s)	Epoch (Number of Iterations)	Mean Squared Error (MSE) values
1	0.05	19	8.091 x 10 ⁻⁷
2	0.06	95	7.886 x 10 ⁻⁷
3	0.29	48	1.036 x 10 ⁻⁶
4	0.34	23	1.149 x 10 ⁻⁶
5	0.4	48	8.931 x 10 ⁻⁷
6	0.54	124	1.031 x 10 ⁻⁶
7	0.71	20	1.196 x 10 ⁻⁶
8	0.95	72	1.008 x 10 ⁻⁶
9	1.42	38	2.289 x 10 ⁻⁶
10	1.89	23	2.852 x 10 ⁻⁶
11	2.36	21	7.479 x 10 ⁻⁶
12	2.84	18	4.311 x 10 ⁻⁶
13	4.73	17	1.029 x 10 ⁻⁶

Table 4.2- Mean squared error (MSE) values for plane 1 (USL=0.09 m/s)

Run	Gas Superficial Velocity, USG (m/s)	Epoch (Number of Iterations)	Mean Squared Error (MSE) values
1	0.05	17	8.661 x 10 ⁻⁷
2	0.06	26	8.926 x 10 ⁻⁷
3	0.29	107	9.631 x 10 ⁻⁷
4	0.34	97	7.758 x 10 ⁻⁷
5	0.4	103	1.195 x 10 ⁻⁷
6	0.54	126	1.073 x 10 ⁻⁷
7	0.71	75	1.079 x 10 ⁻⁶
8	0.95	168	1.619 x 10 ⁻⁶
9	1.42	36	4.180 x 10 ⁻⁶
10	1.89	31	5.532 x 10 ⁻⁶
11	2.36	21	9.903 x 10 ⁻⁶
12	2.84	16	8.150 x 10 ⁻⁶
13	4.73	22	3.745 x 10 ⁻⁶

Table 4.3- Mean squared error (MSE) values for plane 1 (USL=0.14 m/s)

Run	Gas Superficial Velocity, USG (m/s)	Epoch (Number of Iterations)	Mean Squared Error (MSE) values
1	0.05	245	2.350×10^{-7}
2	0.06	180	2.269×10^{-7}
3	0.29	314	4.692×10^{-7}
4	0.34	132	6.325×10^{-7}
5	0.4	299	3.248×10^{-7}
6	0.54	130	4.917×10^{-7}
7	0.71	194	5.171×10^{-7}
8	0.95	84	3.920×10^{-7}
9	1.42	84	5.396×10^{-7}
10	1.89	43	1.430×10^{-6}
11	2.36	30	9.599×10^{-7}
12	2.84	42	1.392×10^{-6}
13	4.73	17	4.123×10^{-7}

Table 4.4- Mean squared error (MSE) values for plane 2 (USL=0.05 m/s)

Run	Gas Superficial Velocity, USG (m/s)	Epoch (Number of Iterations)	Mean Squared Error (MSE) values
1	0.05	101	6.336×10^{-7}
2	0.06	48	7.905×10^{-7}
3	0.29	125	7.334×10^{-7}
4	0.34	56	8.885×10^{-7}
5	0.4	214	7.481×10^{-7}
6	0.54	77	7.520×10^{-7}
7	0.71	151	8.072×10^{-7}
8	0.95	103	1.174×10^{-6}
9	1.42	64	2.288×10^{-6}
10	1.89	30	2.786×10^{-6}
11	2.36	16	6.412×10^{-6}
12	2.84	52	2.782×10^{-6}
13	4.73	64	8.974×10^{-7}

Table 4.5- Mean squared error (MSE) values for plane 2 (USL=0.09 m/s)

Run	Gas Superficial Velocity, USG (m/s)	Epoch (Number of Iterations)	Mean Squared Error (MSE) values
1	0.05	95	7.420×10^{-7}
2	0.06	95	7.122×10^{-7}
3	0.29	95	8.154×10^{-7}
4	0.34	98	9.182×10^{-7}
5	0.4	98	8.644×10^{-7}
6	0.54	96	1.023×10^{-6}
7	0.71	96	9.635×10^{-7}
8	0.95	96	1.956×10^{-6}
9	1.42	92	1.633×10^{-6}
10	1.89	100	6.789×10^{-6}
11	2.36	100	9.763×10^{-6}
12	2.84	93	9.057×10^{-6}
13	4.73	96	4.398×10^{-6}

Table 4.6- Mean squared error (MSE) values for plane 2 (USL=0.14 m/s)

Time series response chart

The time series response plot shows the inputs, targets and errors versus time. It also indicates which time points are selected for training, testing and validation.

Figures 4.10-4.12 below show the time series response charts for planes 1 and 2 at gas and liquid superficial velocities of 0.05 and 0.05-0.14 m/s respectively.

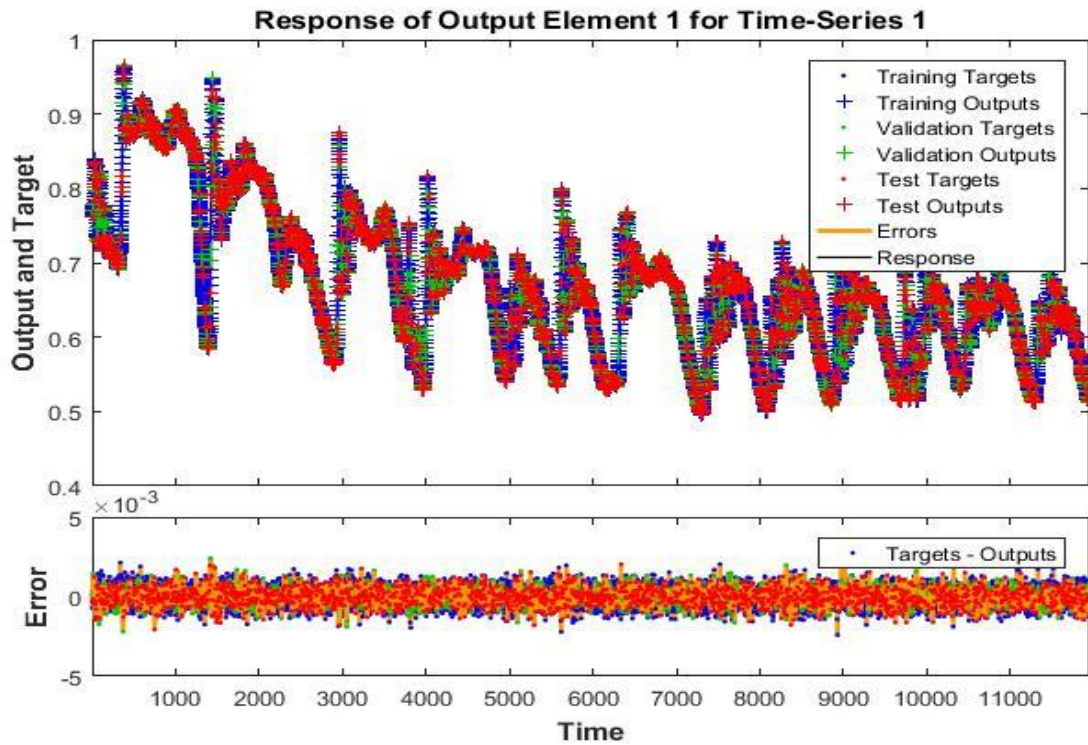


Figure 4.10-Time series plot for plane 1 ($USL=0.05$ m/s and $USG=0.05$ m/s)

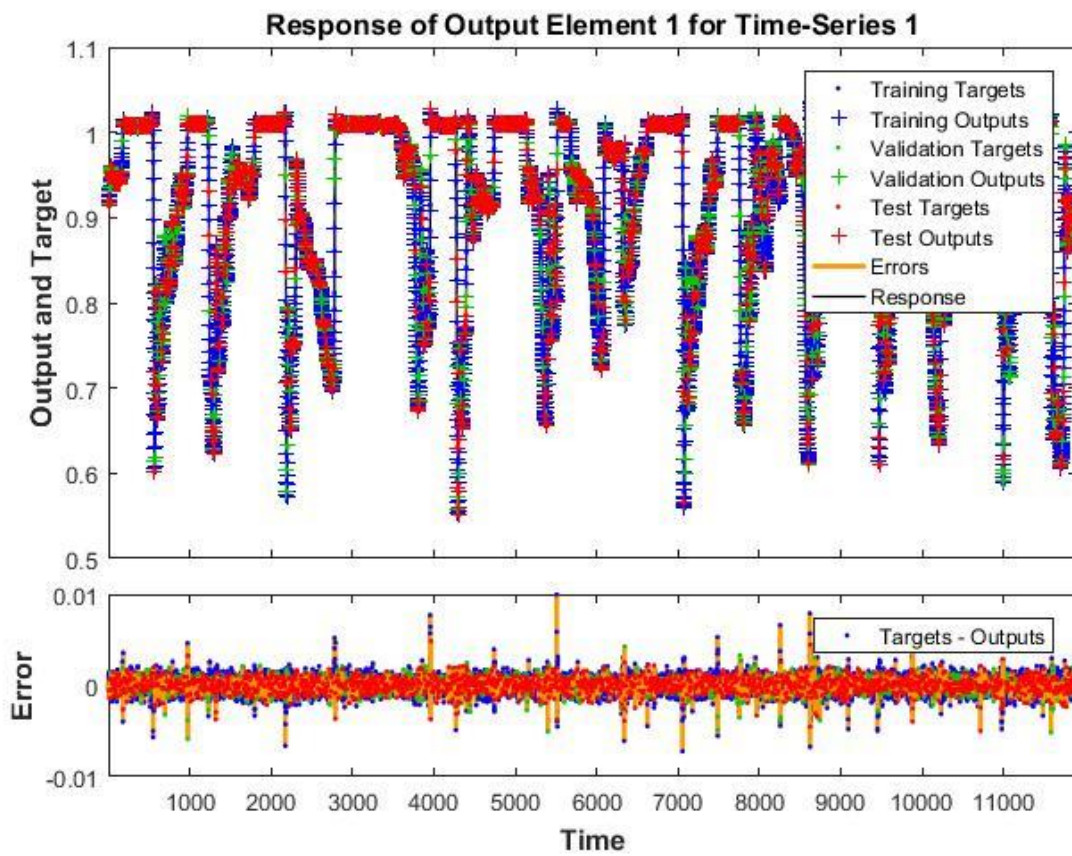


Figure 4.11- Time series plot for plane 1 ($USL=0.09$ m/s and $USG=0.05$ m/s)

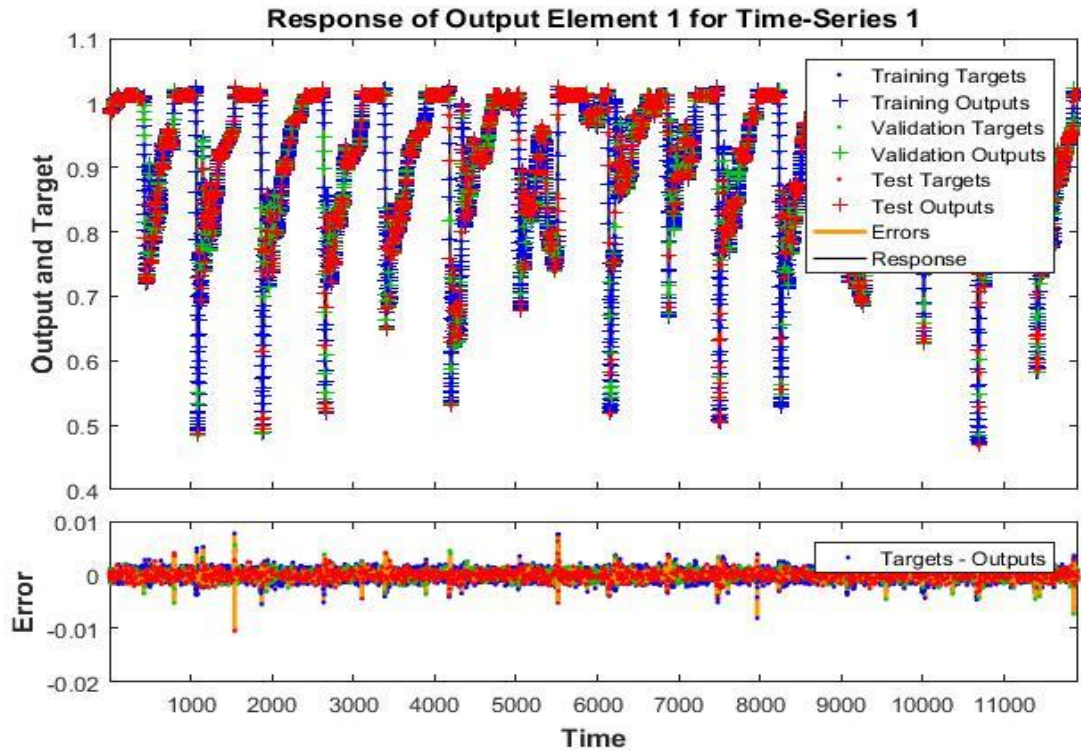


Figure 4.12- Time series plot for plane 1 ($USL=0.14$ m/s and $USG=0.05$ m/s)

4.2. Analysis based on average liquid holdup

To further assess the neural network's efficiency, the average liquid holdup was calculated for both the experimental and simulated runs. Tables 4.7-4.12 below show the calculated values of average liquid holdup for experimental and simulated runs for both planes. A close similarity between the experimental and simulated values is observed for all cases considered. Same values of average liquid holdup are also seen for some cases. This shows that the neural network has successfully predicted the liquid holdup after training with high accuracy.

Run	Gas superficial velocity, USG (m/s)	Average Liquid Holdup (experimental)	Average Liquid Holdup (simulated)
1	0.05	0.672	0.671
2	0.06	0.611	0.611
3	0.29	0.498	0.498
4	0.34	0.486	0.487
5	0.4	0.437	0.438
6	0.54	0.331	0.332
7	0.71	0.342	0.343
8	0.95	0.270	0.270
9	1.42	0.209	0.207
10	1.89	0.180	0.180
11	2.36	0.199	0.199
12	2.84	0.182	0.183
13	4.73	0.222	0.222

Table 4.7- Average liquid holdup for experimental and simulated run(s) for plane 1 (USL=0.05 m/s)

Run	Gas superficial velocity, USG (m/s)	Average Liquid Holdup (experimental)	Average Liquid Holdup (simulated)
1	0.05	0.921	0.922
2	0.06	0.891	0.892
3	0.29	0.649	0.651
4	0.34	0.599	0.599
5	0.4	0.573	0.574
6	0.54	0.489	0.490
7	0.71	0.454	0.454
8	0.95	0.405	0.405
9	1.42	0.267	0.268
10	1.89	0.271	0.272
11	2.36	0.235	0.235
12	2.84	0.253	0.253
13	4.73	0.282	0.282

Table 4.8- Average liquid holdup for experimental and simulated run(s) for plane 1 (USL=0.09 m/s)

Run	Gas superficial velocity, USG (m/s)	Average Liquid Holdup (experimental)	Average Liquid Holdup (simulated)
1	0.05	0.924	0.924
2	0.06	0.912	0.913
3	0.29	0.698	0.698
4	0.34	0.653	0.655
5	0.4	0.619	0.619
6	0.54	0.547	0.543
7	0.71	0.496	0.492
8	0.95	0.416	0.417
9	1.42	0.317	0.317
10	1.89	0.260	0.260
11	2.36	0.249	0.248
12	2.84	0.258	0.258
13	4.73	0.293	0.293

Table 4.9- Average liquid holdup for experimental and simulated run(s) for plane 1 (USL=0.14 m/s)

Run	Gas superficial velocity, USG (m/s)	Average Liquid Holdup (experimental)	Average Liquid Holdup (simulated)
1	0.05	0.684	0.683
2	0.06	0.619	0.619
3	0.29	0.507	0.507
4	0.34	0.499	0.499
5	0.4	0.450	0.450
6	0.54	0.348	0.349
7	0.71	0.285	0.285
8	0.95	0.356	0.356
9	1.42	0.226	0.226
10	1.89	0.194	0.194
11	2.36	0.211	0.212
12	2.84	0.197	0.197
13	4.73	0.222	0.222

Table 4.10- Average liquid holdup for experimental and simulated run(s) for plane 2 (USL=0.05 m/s)

Run	Gas superficial velocity, USG (m/s)	Average Liquid Holdup (experimental)	Average Liquid Holdup (simulated)
1	0.05	0.939	0.939
2	0.06	0.910	0.911
3	0.29	0.669	0.671
4	0.34	0.620	0.621
5	0.4	0.594	0.595
6	0.54	0.512	0.513
7	0.71	0.470	0.471
8	0.95	0.422	0.422
9	1.42	0.291	0.292
10	1.89	0.295	0.295
11	2.36	0.257	0.257
12	2.84	0.277	0.278
13	4.73	0.304	0.304

Table 4.11- Average liquid holdup for experimental and simulated run(s) for plane 2 (USL=0.09 m/s)

Run	Gas superficial velocity, USG (m/s)	Average Liquid Holdup (experimental)	Average Liquid Holdup (simulated)
1	0.05	0.925	0.924
2	0.06	0.91	0.91
3	0.29	0.698	0.698
4	0.34	0.651	0.653
5	0.4	0.619	0.619
6	0.54	0.548	0.544
7	0.71	0.497	0.493
8	0.95	0.420	0.420
9	1.42	0.329	0.329
10	1.89	0.264	0.265
11	2.36	0.253	0.252
12	2.84	0.263	0.262
13	4.73	0.291	0.290

Table 4.12- Average liquid holdup for experimental and simulated run(s) for plane 1 (USL=0.14 m/s)

An analysis of the effect of the gas and liquid superficial velocity on liquid holdup was also carried out for both planes 1 and 2.

Figures 4.13 and 4.14 show the effect of liquid and gas superficial velocities on liquid holdup for the experimental and simulated data respectively. The figures show a decreasing trend with increasing gas superficial velocity. On the other hand, the liquid holdup increases with an increase in liquid superficial velocity. Increasing the gas superficial velocity implies an increase in the gas flowrate. This results in an increase in the residence time of the gas phase in the system and consequently, a reduction in the values of the liquid holdup.

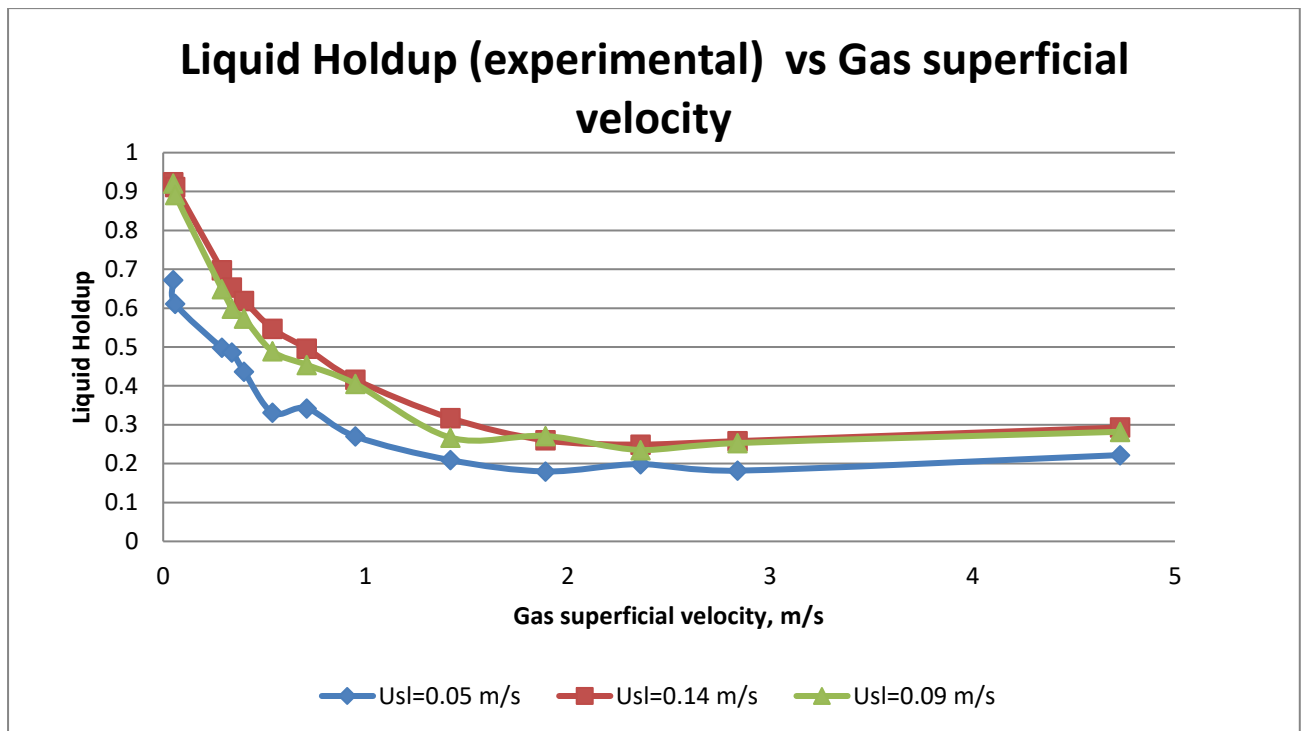


Figure 4.13- Plot of Liquid Holdup versus Gas superficial Velocity (experimental)

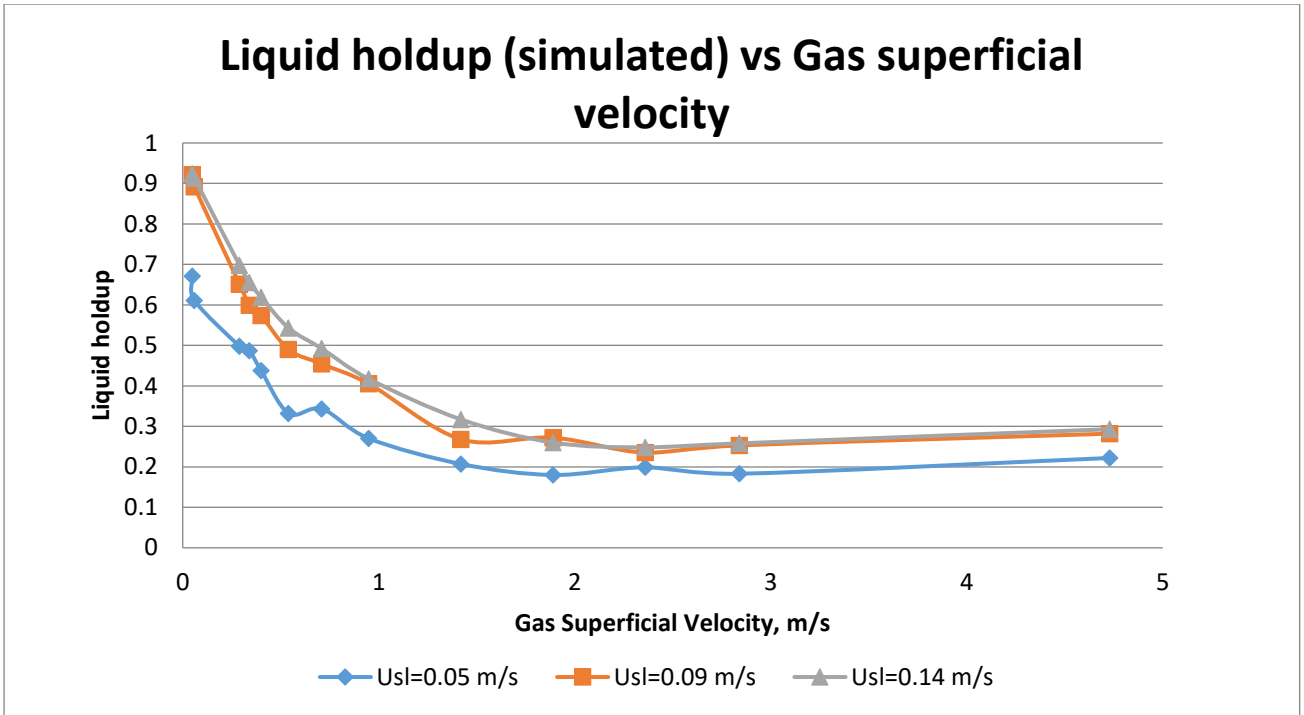


Figure 4.14- Plot of Liquid Holdup versus Gas Superficial Velocity (simulated)

4.3. Analysis based on structural velocity and frequency

Computational macros were used for the determination of the structural velocity and frequency for each run (experimental and simulated). A cross plot of simulated structural velocity versus the experimental structural velocity is presented in the Figure 4.15 below. A 100 percent efficiency of the neural network is observed for a liquid superficial velocity of 0.05 m/s. A slight difference is noticed for liquid and gas superficial velocities of (0.09, 0.14) and (2.36, 1.42) m/s respectively.

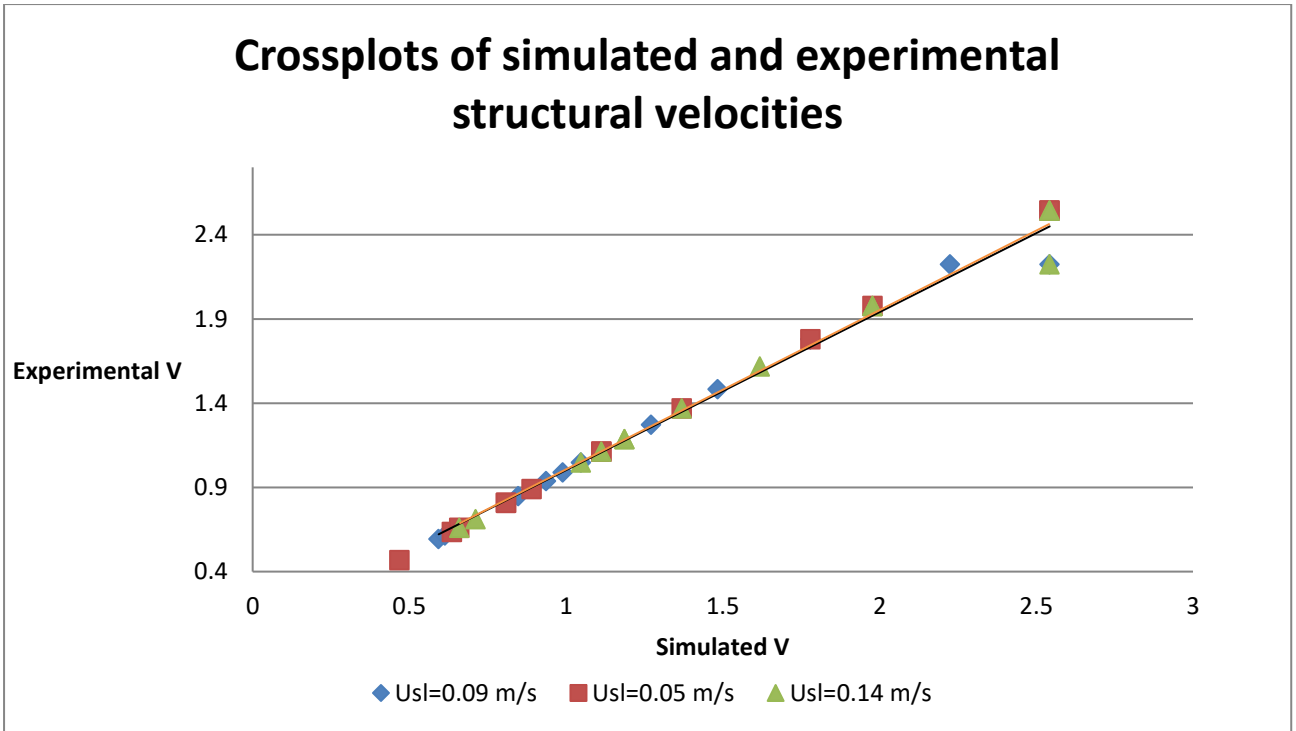


Figure 4.15- Cross plot of simulated and experimental structural velocities.

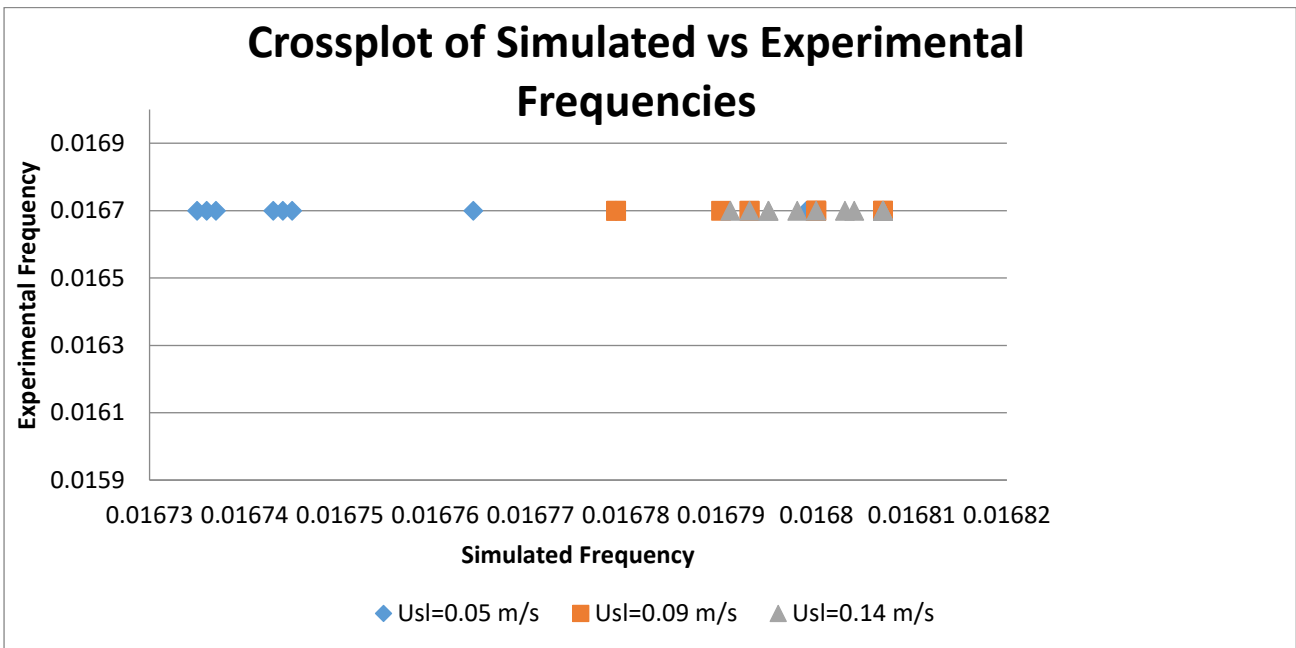


Figure 4.16- Crossplot of experimental and simulated frequencies

The effect of liquid and gas superficial velocities on structural velocity and frequency were carried out. The results of this analysis are presented in Figures 4.15-4.16.

It is noticed that the structure velocity increases with an increase in the liquid superficial velocity. At higher liquid superficial velocity, the bubbles move faster and thus, the increase in structure velocity as liquid superficial velocity is increased.

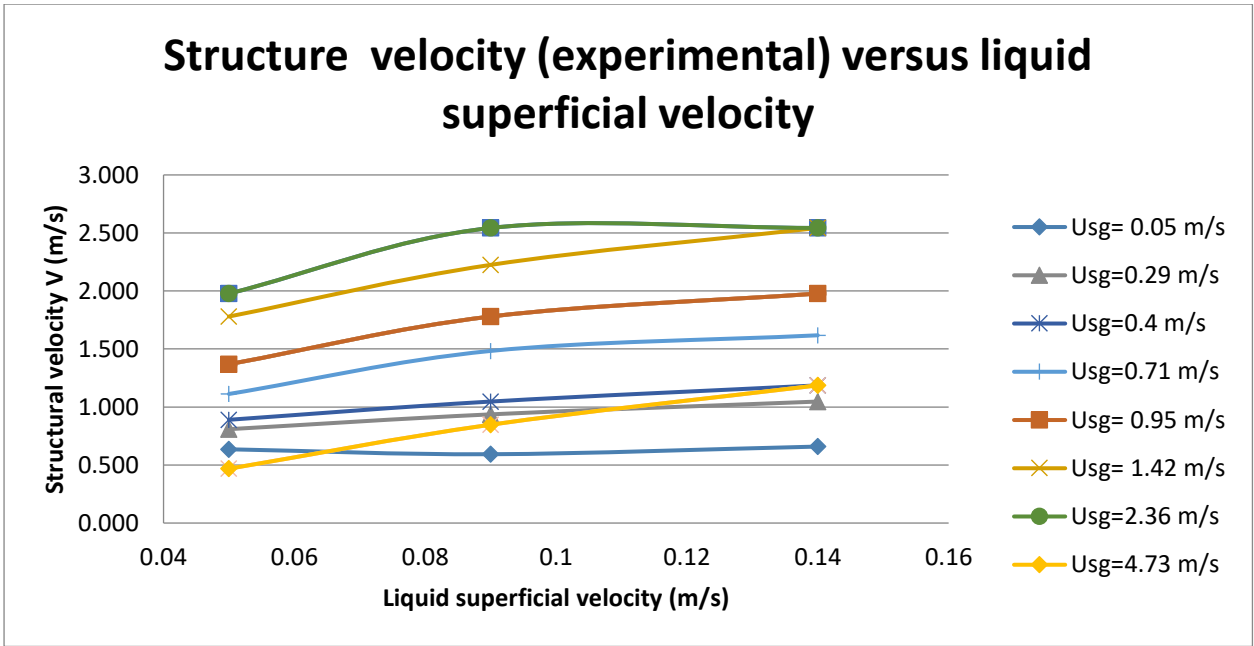


Figure 4.17- Plot of Structural velocity (experimental) versus Liquid superficial velocity

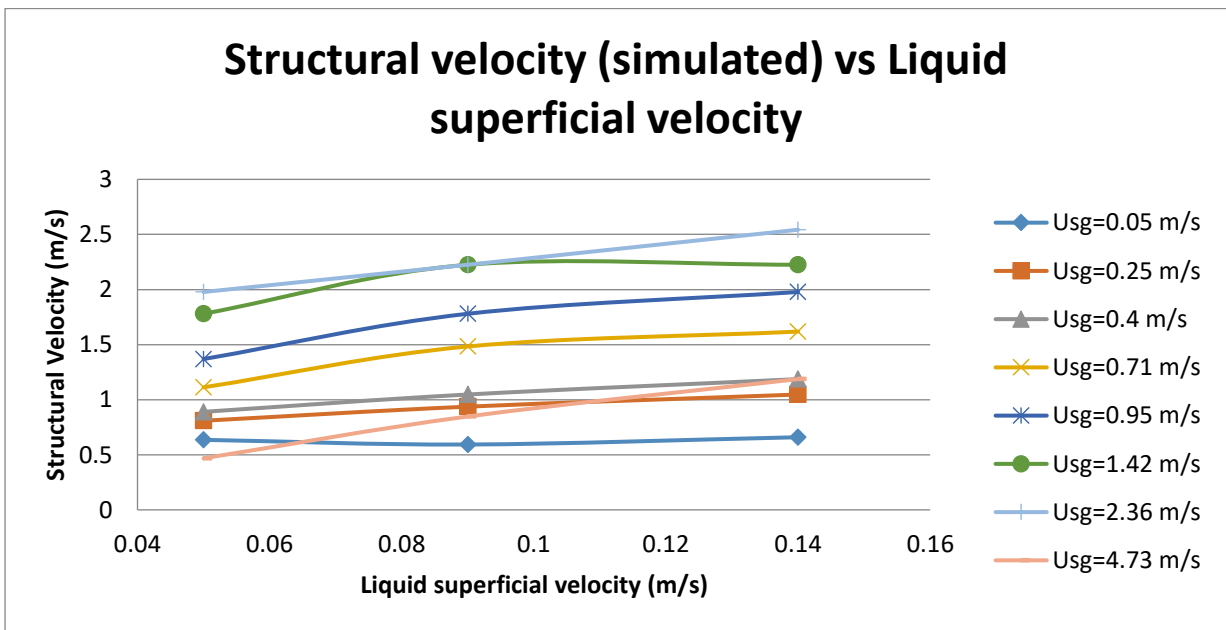


Figure 4.18- Plot of Structural velocity (simulated) versus Liquid superficial velocity

CHAPTER 5

5.0. CONCLUSIONS AND RECOMMENDATIONS

5.1. CONCLUSIONS

In this research, the use of neural network was applied to predict liquid holdup during slug flow for a horizontal pipe orientation. This was achieved by training the neural network using the experimental data provided. The “Nonlinear Autoregressive with External (Exogenous) Input” solution for non-linear series problem was selected for this study. The experimental data contained values of liquid holdup measured at different time interval and at two different planes located at the upper and lower parts of the system for an air-silicone oil two phase system. The liquid holdup was measured at varying gas and liquid superficial velocities. The results obtained were validated through the use of MATLAB charts and compared with experimental data. Average liquid holdup, translational bubble velocity (structure velocity) and frequency were used as basis of comparison during analysis the result obtained.

The effect of gas and liquid superficial velocities on the bubble velocity and slug frequency was also investigated.

It can be concluded from this study that:

1. The neural network successfully predicted the liquid holdup with high accuracy. This is the case as the experimental and simulated values of average liquid holdup, structure velocity and frequency were closely similar and even exact in some cases. The efficiency of the neural network is also evident from the cross plots of experimental and simulated values of structure velocity and frequency.
2. To accurately predict liquid holdup using the neural network tool, a minimum of 50 epochs (number of iteration) and a maximum of 10 delays should be set as the neural network architecture.
3. The liquid holdup is largely dependent on gas and liquid superficial velocity. It decreases with increasing gas superficial velocity and increases with liquid superficial velocity.
4. The structure velocity increases with increasing gas and liquid superficial velocities.

5.2 RECOMMENDATIONS

The application of artificial neural network in the oil and gas industry can assist in solving commonly encountered problems in the industry. It should therefore be more explored than it currently is. Its ability to accurately predict parameters within a short time frame can be extensively researched and improved on. Prediction of more parameters besides liquid holdup could be researched. Other flow patterns besides slug flow for the horizontal pipe orientation

could be explored. Training algorithms could be researched on to determine which is more effective in generating accurate results. Network architecture such as number of delays and number of iterations could be extensively researched on to determine the best combination of the two for running the neural network.

The efficiency of the neural network could also be tested for systems where other parameters besides gas and liquid superficial velocities are varied.

Exploring all these areas would assist in understanding the use of neural networks for predictions thereby ensuring its efficiency when applied to solve problems.

REFERENCES

1. Al-Safran, E. (2009). Prediction of slug liquid holdup in horizontal pipes. *Journal of Energy Resources Technology, Transactions of the ASME*, 131(2), 0230011–0230018. <https://doi.org/10.1115/1.3120305>
2. Anumbe, N. C., & Khan, J. (2018). Experimental investigation of two-phase (gas/liquid) flow in intermediate sized, horizontal and inclined pipes. 231. <https://scholarcommons.sc.edu/etd>
3. Bagci, S., & Al-Shareef, A. (2003). Characterization of Slug Flow in Horizontal and Inclined Pipes. *Proceedings - SPE Production Operations Symposium*, 539–548. <https://doi.org/10.2523/80930-ms>
4. Beers, B., & Westfall, P. (2020, February 19). Regression Definition. <https://www.investopedia.com/terms/r/regression.asp>
5. Beggs, D., & Brill, J. P. (1973). A study of Two-Phase Flow in Inclined Pipes.
6. Dukler, A. E. (1986). Flow Pattern Transitions in Gas-liquid Systems : Measurement and Modeling. 1–2.
7. Frankenfield, J. (2019, July 19). Predictive Modeling Definition. <https://www.investopedia.com/terms/p/predictive-modeling.asp>
8. Frankenfield, J. (2021). Artificial Intelligence (AI) Definition. <https://www.investopedia.com/terms/a/artificial-intelligence-ai.asp>
9. Gershenson, C. (2003). Artificial Neural Networks for Beginners. 1–8.
10. Granados-C., J., & Camacho-V., R. (1998). Analysis of two-phase flow in horizontal and inclined pipes with mechanistic models. *Proceedings of the SPE International Petroleum Conference & Exhibition of Mexico*, 2(2), 221–226. <https://doi.org/10.2523/39857-ms>
11. Halton, C. (2019, July 19). Predictive Analytics Definition. <https://www.investopedia.com/terms/p/predictive-analytics.asp>
12. Harvey, S., & Harvey, R. (1998). An introduction to artificial intelligence. *Appita Journal*, 51(1). <https://doi.org/10.2514/6.1994-294>
13. Inzaugarat, E. (2018). Understanding Neural Networks: What, How and Why? | by Euge Inzaugarat | Towards Data Science. <https://towardsdatascience.com/understanding-neural-networks-what-how-and-why-18ec703ebd31>

14. Kuldeep, S., & Anitha, G. S. (2017). Neural Network Approach for Processing Substation Alarms. October 2015.
15. Luhaniwal, V. (2019). Analyzing different types of activation functions in neural networks — which one to prefer? | by vikashraj luhaniwal | Towards Data Science. <https://towardsdatascience.com/analyzing-different-types-of-activation-functions-in-neural-networks-which-one-to-prefer-e11649256209>
16. Mandhane, J., Gregory, G., & Aziz, K. (1974). A Flow Pattern Map for Gas-Liquid Flow in Horizontal Pipes. *International Journal of Multiphase Flow*, 1, 537–553.
17. Mayo, M. (2017). Neural Network Foundations, Explained: Updating Weights with Gradient Descent & Backpropagation - KDnuggets. <https://www.kdnuggets.com/2017/10/neural-network-foundations-explained-gradient-descent.html>
18. Purvis, D. C., & Kuzma, H. (2016). Evolution of uncertainty methods in decline curve analysis. *SPE Hydrocarbon Economics and Evaluation Symposium*, 2016-Janua(May), 17–18. <https://doi.org/10.2118/179980-ms>
19. Shippen, M. E., & Scott, S. L. (2004). A neural network model for prediction of liquid holdup in two-phase horizontal flow. *SPE Production and Facilities*, 19(2), 67–76. <https://doi.org/10.2118/87682-PA>
20. Shukla, M., & Abdelrahman, M. (2004). Artificial Neural Networks Based Steady State Security Analysis of Power Systems. 266–269.
21. Taitel, Y., & Dukler, A. . (1976). A Model for Predicitng Flow Regime Transitions in Horizontal and Near Horizontal Gas-Liquid Flow. 22(1), 47–55.
22. Theofanous, T. G., & Hanratty, T. J. (2003). Appendix 1 : Report of study group on flow regimes in multifluid flow q. 29, 1061–1068. [https://doi.org/10.1016/S0301-9322\(03\)00079-X](https://doi.org/10.1016/S0301-9322(03)00079-X)
23. Vrahatis, M. N., Magoulas, G. D., Parsopoulos, K. E., & Plagianakos, V. P. (2001). Introduction to Artificial Neural Networks and Applications. *Proceedings of the Neuroscience 2000 Conference*, November 2014, 1–12. <https://doi.org/10.13140/2.1.1755.2322>
24. Weisman, J., & Kang, S. . (1981). Flow pattern transitions in vertical and upwardly inclined lines. 9, 271–291.
25. Xiao, R., Li, K., Sun, L., Zhao, J., Xing, P., & Wang, H. (2020). The Prediction of liquid

holdup in horizontal pipe with BP neural network. Energy Science and Engineering, 8(6), 2159–2168. <https://doi.org/10.1002/ese3.655>